AD NUMBER

AD861444

NEW LIMITATION CHANGE

TO

Approved for public release, distribution unlimited

FROM

Distribution authorized to U.S. Gov't. agencies and their contractors; Administrative/Operational Use; AUG 1969. Other requests shall be referred to Commanding General, U.S. Army Electronics Command, Attn: AMSEL-BL-FM-P, Fort Monmouth, NJ.

AUTHORITY

ECOM ltr, 29 Nov 1971

AD

Research and Development Technical Report
ECOM-0396-F

NEW YORK UNIVERSITY
RESEARCH DIVISION
University Heights, Bronx, N.Y. 10453

Department of Meteorology and Oceanography
Geophysical Sciences Laboratory Report No. TR-69-9

ION ANEMOMETER

FINAL REPORT

Covering Period: 17 June 1968 to 31 July 1969

Contract No. DAAB-07-68-C-0396

Prepared by

Alan M. Nathan
Leon Bennett
Moises Cytter

August 1969

DISTRIBUTION STATEMENT

This document is subject to special export controls and each transmittal to foreign governments or foreign nationals may be made only with prior approval of CG, U. S. Army Electronics Command, Fort Monmouth, N. J.

Attn: AMSEL-BL-FM-P

ECOM

UNITED STATES ARMY ELECTRONICS COMMAND · FORT MONMOUTH, N.J.

Reports Control Symbol
OSD 1366

Technical Report ECOM-0396-F

New York University
Research Division
University Heights
Bronx, New York 10453

Department of Meteorology and Oceanography
Geophysical Sciences Laboratory Report No. TR-69-9

ION ANEMOMETER

FINAL REPORT

Covering Period: 17 June 1968 to 31 July 1969

Contract No. DAAB-07-68-C-0396

Prepared by

Alan M. Nathan
Leon Bennett
Moises Cytter

August 1969

DISTRIBUTION STATEMENT

This document is subject to special export controls and each transmittal to foreigh governments or foreign nationals may be made only with prior approval of CG, U. S. Army Electronics Command, Fort Monmouth, N. J. Attn: AMSEL-BL-FM-P

for

Atmospheric Sciences Laboratory
Army Electronics Command
Fort Monmouth, New Jersey

ACKNOWLEDGEMENTS

The helpful cooperation and technical assistance rendered this program by Mr. Marvin Lowenthal, Mr. Andrew Petriw and Dr. Reinhold Marchgraber, all of the Atmospheric Sciences Laboratory, U. S. Army Electronics Command, Fort Monmouth, New Jersey, are gratefully acknowledged.

CONTENTS

1. Abstract

An ion anemometer is described that is designed to measure one vector component of air velocity in the range from 0 to 120 cm/sec. The instrument's electrical output signal is a measure of the magnitude of the projection of the instantaneous wind vector onto the instrument's single axis of sensitivity. Ganging of more than one device permits the determination of two or three vector components of the wind velocity.

The instrument employs a radioactive source of alpha particles to ionize the air molecules in a small region between two oppositely charged electrodes. The equal numbers of positive and negative ions generated at a constant rate are separately collected by the two charged electrodes. In the absence of wind, the potential due to space charge is zero at the electrical midpoint between the two collecting electrodes where an electrical probe is situated. Any wind component along the axis, however, causes an unbalance which is sensed by a small current in the probe that is amplified and recorded.

This development effort differs from prior work in its concentration on the following goals: 1) linear output with velocity, 2) a true cosine law response to an off-axis airstream, 3) a usefully large analog signal capable of simple readout at very low wind speeds.

consider an arrangement of two parallel planar electrodes at a potential difference of several hundred volts with a source of ions between the plates. With zero wind, almost all ions will be collected by the electrodes and the ammeter will read a maximum current. As the wind velocity increases, fewer and fewer ions will be collected as the ion trajectories are increasingly modified by the wind vector. Thus measured ion current will vary with the wind.

A similar ion anemometer designed with approximate spherical symmetry so as to be non-directional in its response to wind was described in 1949* and ion transit tine instruments have been used in the past**. Yet no generally useful field instrument has been developed to date. It is clear that certain difficulties have prevented greater use of the ion concept in the area of accurate wind measurements.

These difficulties include: 1) Small output (typically 10^{-9} amps) and the associated problems of amplifier stability and response time. 2) Lack of geometry supplying both a linear response to velocity and a directional cosine law response to a yawing wind. While each has been demonstrated individually, the literature does not report a suitable combination. 3) Undesirable instrumental sesnitivity to varying ambient conditions, (pressure, temperature, humidity) and source intensity decay. 4) Calibration uncertainties, i.e., developing a standard to be used in testing an instrument generally beyond state of the art devices. 5) Lack of comprehensive theoretical treatment of ion trajectory as a function of instrumental parameters.

In what follows, we report progress in overcoming the above difficulties

---

* Lovelock, J.E. and Wasilewska, E.M., "An Ionization Anemometer," J. Scientific Instruments, Vol. 26, 1949, p. 367.

** Straub, L.G. Ripken, J.E., and Killen, J.M., "Research and Development Studies for a Low Level Wind Measuring System," Univ. of Minn., Project Report No. 49, 1955.

in the case of a projected field instrument designed for meteorological observations of low air velocities. The approach is one stressing a fundamental examination of the ion anemometer combined with an intensive experimental evaluation. While effort is focused on an ultimate working device, the immediate concern is with background research rather than detail final design. Many of the above listed difficulties have been surmounted; however, certain problems remain. Thus, this program may be viewed as a step towards the development of a successful device for the measurement of the vector components of low velocity winds.

3. Ion Anemometer Design Analysis Considerations

A. Ion Production in Air

A given radioactive isotope, such as Polonium 210, emits alpha particles (He_4^{++}) at a constant rate. All the alphas are emitted with a constant characteristic energy and as they travel they cause intense ionization of the gas molecules in their path, typically about 10^5 ion pairs are created per cm. They lose energy at a fairly constant rate per cm., due to the ionization they produce so that they all come to a stop after traveling a short distance, typically several cm. Their range in air is quite constant and characteristic of their original energy.

The electrons produced very quickly attach themselves to gas molecules giving rise to negative ions equal in number and total charge to the positive ions generated by the original collisions. In air, these ions have lifetimes ranging from seconds to minutes. In the presence of electric fields, the ions will be accelerated towards electrodes whose charge is opposite to their own, i.e., positive towards a negative electrode and negative ions toward a positive electrode.

B. Ion Trajectories

The ion anemometer concept described in this report is based on the following elementary physical considerations:

1. Ions in air will reach an average terminal velocity in a negligibly short time when accelerated by a local electric field. This fact results from the large numbers of collisions with neutral air molecules which they experience, on the order of 10^9 per second.
2. Positive ions will move in the direction of the electric field vector $\vec{E}$ and negative ions in the $-\vec{E}$ direction. Ion terminal

vector velocities are given by the following equations (for singly charged ions):

$$\vec{v}^{+} = \mu^{+}\vec{E} \quad , \quad \vec{v}^{-} = -\mu^{-}\vec{E} \qquad (1)$$

where $\mu^{\pm}$ is the ion mobility constant for $\pm$ ions in cm/sec/volt/cm. Many studies on natural and artificially produced air ions have shown that the mobility $\mu^{\pm}$ is actually given by $k^{\pm}/P$, where P is air pressure and $k^{\pm}$ is the mobility coefficient, a constant which is slightly larger for negative ions than for positive. Published data* shows $k^{\pm}/P$ to be approximately 2 cm/sec/volt/cm for negative ions and about 25 percent less for positives.

3. Since ambient wind moves the air parcel in which an ion is imbedded, the actual velocity of any ion is given by the following vector equation:

$$\vec{v}^{\pm} = \pm\left(\mu^{\pm}\vec{E}\right) + \vec{W} \qquad (2)$$

4. By definition $\vec{E} = -\text{grad}\, V$ or (3)

$$\vec{E} = -\left[\vec{i}\frac{\partial V}{\partial x} + \vec{j}\frac{\partial V}{\partial y} + \vec{k}\frac{\partial V}{\partial z}\right]$$

Therefore any change in the total potential between electrodes (V) will alter $\vec{E}$ in magnitude, but not in direction.

5. Therefore, if the wind vector, $\vec{W}$, changes with time it should be possible to buck out the effect of this change on ion trajectories by a compensating change in electrode voltages.

---

* "Advances in Electronics and Electron Physics," Vol. 19, 1964, Academic Press, p. 178.

3. Ion Anemometer Design Analysis

To design a useful ion anemometer which will exploit the above physical considerations, consider as a possibility the following idealized arrangement. Two plane parallel mesh electrodes of large area (approximately infinite planes) face each other at distances -L and R respectively from a center electrode or "probe" at x = 0. The left and right outer electrodes or "collector" electrodes are connected respectively to the negative and positive terminals of a high voltage supply (2000 volts). The probe is connected through a sensitive current meter to a grounded, variable tap on a potentiometer which spans the high voltage supply. By this means, the potential of the probe may be varied $\pm$ with respect to the electrical midpoint between the two outer electrodes.

A radioactive source of alpha particles is assumed to be arranged symmetrically in or near the center probe so that a constant rate of ion pair generation occurs in the region between the L and R electrodes. In other words, we assume a uniform constant number of ion pairs generated per unit volume per unit time within the electrodes and none generated outside. (If ion pairs are produced outside the two planar electrodes, it can be shown from Kirchoff's laws that all resulting currents cancel out.)

Under the above assumed conditions, all positive ions will migrate from right to left in the uniform field between the positive R electrode and the negative L electrode. Negative ions will of course migrate from left to right. Thus we have a net positive current to the left collector and a net negative current to the right electrode.

At any coordinate, X, the positive ion current density (amperes/cm^2) must be equal to the product of the constant ion generation rate per unit

volume, N, times the distance from R to X. Thus,

$$j_x^+ = Ne(R-X) \tag{4}$$

where e = charge on an electron.

This is so because of continuity and chage conservation which demand that all positive ions generated per second to the right of any plane at coordinate X, must be swept leftward across this plane by the electric field, otherwise charges would continuously accumulate to the right of the plane at X. (we have tacitly assumed that any current to the probe is negligible in comparison with the currents to the collector electrodes and that the presence of the probe does not alter the field between the two collector electrodes.)

By the same argument, the negative ion current density is

$$j_x^- = Ne(L+X) \tag{5}$$

But by definition, current density is given by

$$|j_x| = \rho_x |v_x| \tag{6}$$

where ρ_x = charge density in coulombs/cm^3.

and v_x = local charge velocity

Therefore, we can solve for the charge densities at coordinate X thus,

$$\rho_x^+ = Ne(R-X)/|\vec{v}_x^+|$$
$$\rho_x^- = Ne(L+X)/|v_x^-| \tag{7}$$

It is now possible to apply Poisson's equation as follows

$$\epsilon_0 \frac{d^2V}{dx^2} = -\rho_x = (\rho_x^- - \rho_x^+) \tag{8}$$

or by substituting equation (5)

$$\epsilon_0 \frac{d^2V}{dx^2} = Ne\left[\frac{(L+x)}{|\vec{v}_x^-|} - \frac{(R-x)}{|\vec{v}_x^+|}\right] \tag{9}$$

From equation (2) we have that

$$\begin{aligned} |\vec{v}_x^-| &= \mu^- |E_x| + W = \mu^- \frac{dV}{dx} + W \\ |\vec{v}_x^+| &= \mu^+ |E_x| - W = \mu^+ \frac{dV}{dx} - W \end{aligned} \tag{10}$$

and

where we have assumed that W is in the + x direction.

Thus upon substitution of (10) in (9) we get finally,

$$\epsilon_0 \frac{d^2V}{dx^2} = Ne\left[\frac{(L+x)}{\mu^- \frac{dV}{dx} + W} - \frac{(R-x)}{\mu^+ \frac{dV}{dx} - W}\right] \tag{11}$$

This differential equation describes the potential distribution in the ion space charge cloud between the two collector electrodes. If it could be solved then one could deduce the potential at x = 0 where the probe is placed and thereby determine probe unbalance as a function of wind and the system voltages and geometry.

Unfortunately, the equation is nonlinear and all efforts at an analytic solution to date have failed. We can, however, demonstrate a somewhat over-simplified physical analysis of device performance based on the foregoing model.

We assume first that $W = 0$ and that $\frac{dV}{dx}$ is approximately constant across the space between the outer electrodes. This assumption is not too unrealistic

since the effect of the ion space charge can be shown to be small in comparison with the 2000 volts applied, ($\approx$ 10 percent). Then equation (5) predicts that the net charge is distributed as shown below,

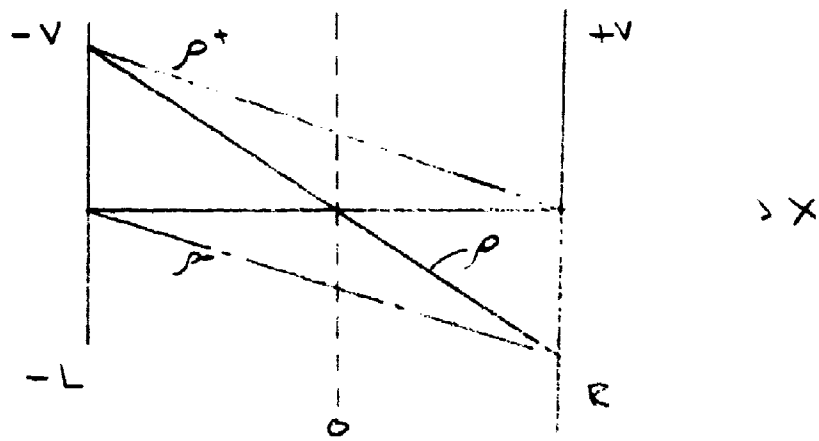

It then follows that $\frac{d^2V}{dx^2}$ and $\frac{dV}{dx}$ are as plotted below.

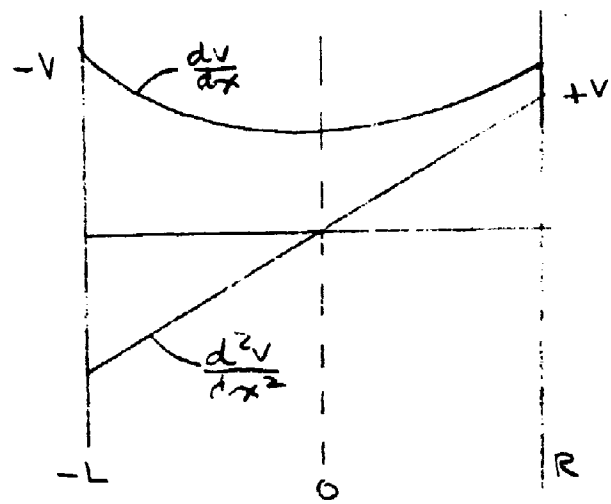

Accordingly, with $W=0$, we can plot V(x) as shown below

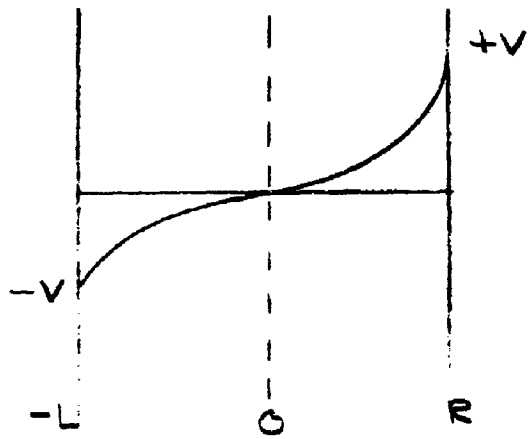

Note that V(x) = 0 at x = 0 where the probe is located.

If now, we let $W>0$, then v_x^+ is decreased while v_x^- is increased, so that the plot of charge distribution is altered, becoming

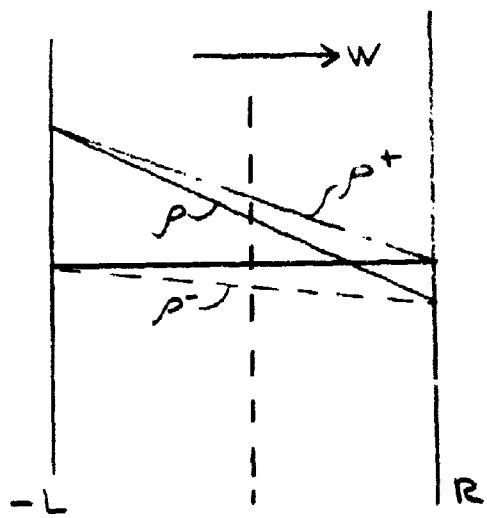

Therefore we must alter the plot of $\frac{d^2V}{dx^2}$ and $\frac{dV}{dx}$ as shown

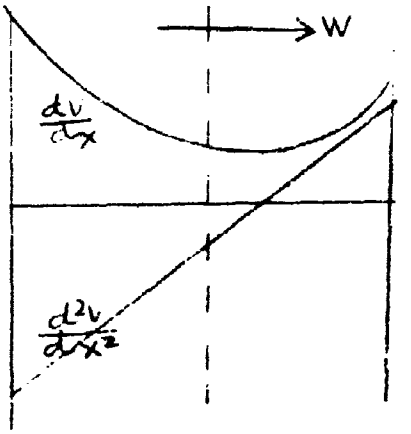

And finally se see that $V(x)$ has been altered by the wind as follows.

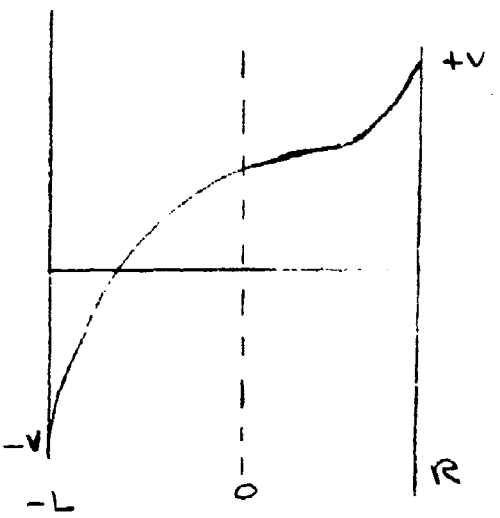

It is clear that the probe is now located at a point in the space charge cloud where the potential has been raised above zero because of the wind. Since the probe ground return is still midway between -V and +V, or zero, it will draw some + unbalance current, whose magnitude will be proportional in some sense to the wind. By the same token, if we move its ground returns toward +V, we thereby balance out the unbalance current since there is no longer any potential difference between the point where the probe is in contact with the space charge and its return to the potentiometer tap.

These qualitative conclusions are in complete accord with the observed behavior of the ion anemometer in that they predict the correct sign for unbalance signals as they have been observed. Furtheremore, they imply an equivalence between unbalance current and the nulling voltage offset, as observed.

D. Aerodynamic and Blockage Considerations

1. Supporting Blockage

The sensing portion of the ion anemometer must be supported relative to the ground, through use of structural members. Such members must inevitably block or interfere with the flow of air from one or more directions. The design problem is one of minimizing the error so produced.

A real fluid, in traversing an obstacle, will produce a wake, or region of increased vorticity. Within the wake, velocities are lower than those of the free stream and the turbulence level higher. Minimizing wake influence on the ion anemometer is the desired goal.

Wake characteristics do not lend themselves readily to theoretical treatment; conventional potential flow aerodynamics, which stipulate irrotational flow, is not sufficiently accurate in handling the large vorticity wake. Boundary layer theory, in which the permissible vorticity is unbounded, has been successfully applied to a number of simple wake cases. However, as such results are typical numerical solutions to a series of partial differential equations, general applicability is limited. Therefore, current approaches to the wake stress a combination of empirical results with limited theoretical guidance.

Wake characteristics are functions of the Reynolds number (Re) of the event and the geometry of the obstacle. For a small Re (say $\lesssim$ 5) the wake is thread-like. At Re = 5 $\longrightarrow$ 40 a broad laminar wake results, one that is quite stable. From Re = 40 $\longrightarrow$ 300 the wake is essentially a Karman street vortex system, evidencing instability of the main vortices. In a similar manner, each successively higher Re range has its own attributes.

The influence of the obstacle geometry is also highly significant. A streamlined (i.e., limited flow separation) obstacle will typically produce

a narrow wake of great persistence. Such a wake, while physically small, will mix but slightly with the free stream. Consequently the wake effect will persist for many tens of obstacle diameters downstream. Conversely, a bluff obstacle (one with severe separation characteristics) will create a large wake with a powerful mixing characteristic. Thus the bluff object wake will generally "dissipate" in a shorter distance downstream than the streamlined object wake.

In other words, both streamlined and bluff supports have certain disadvantages. The bluff support will typically affect the ion anemometer through a larger angle of wind yaw than the streamlined support; however, the magnitude of the effect, taken on the wake axis at equivalent distances downstream, is generally larger for the streamlined support.

The Re value may be obtained from the approximation:

Re = velocity (MPH) X obstacle major dia. (inch) x 780.

For a one MPH wind, the Re is about 800 per inch of obstacle major diameter. Practical sized supports yield Re of the order of magnitude "hundreds." The region 150 $\longrightarrow$ 130,000 is termed the "subcritical." The wake is essentially laminar, although it contains cochlear vortices. Wind tunnel measurements* of the wake characteristics of various bluff bodies (blunt nosed cones, hemispheres) at the upper end of this Re range, indicate an on-axis dynamic pressure recovery of approximately 0.8 at a downstream distance equal to six object diameters. More streamlined objects (bullet with boat tail base) achieve the same dynamic pressure recovery in about ten object diameters. Noting that the dynamic pressure is proportional to the square of velocity, it follows that the velocity recovery corresponding to the 0.8 pressure level

---

* Theoretical Parachute Investigations, Anonymous, Prog. Rept. No. 17, Dept. of Aero Engr'g., U. of Minn., 1961, AD 605 143

is approximately 0.9. Thus at a wake distance equal to 6 $\longrightarrow$ 10 object diameters the on-axis velocity drop will be about 10 percent, as compared to the free stream in the Re regime of interest. Off-axis wake velocity reductions will be smaller than the figures given; the distribution of wake velocity with distance across the wake axis is given by Gauss' function.

The wake created by a circular cylinder has been explored at length* using numerical methods. At an Re of 320 (roughly corresponding to a 1 cm. diameter at 1 MPH), standing vortices are generated immediately behind the cylinder to a distance of less than three cylinder diameters. Beyond this point, pressure recovery is at least equal to 90 percent of the free stream value, at all points (on-axis and off-axis) in the wake. It follows that the velocity decrement beyond three cylinder diameters at the stated Re is less than 5 percent. Further reduction of the velocity decrement is asymptotic**, according to the relation $\Delta V = K/\sqrt{\text{distance}}$.

To summarize, if 5 $\longrightarrow$ 10 percent velocity reduction error is considered acceptable the anemometer supports, if cylindrical in form, should be at least three cylinder diameters removed from the test zone. For a comparable error, at least 6 $\longrightarrow$ 10 percent diameters distance from the test zone are required if the obstacle is more streamlined in form than a cylinder, or if the object generates a large Re.

These minimum values of support distance have been generally followed in the final design of the ion anemometer, with one major exception - the placement of the amplifier. Considerations of signal wire length have forced an amplifier location much closer to the test zone than desired aerodynamically.

---

* "The Steady Flow of a Viscous Fluid Plast a Circular Cylinder, Dennis, S.C.R., and Shimshoni, M., Aero. Res. Council, U.K. No. 26, 104, Aug. 1964, AD 450 760.

** "Boundary Layer Theory," Schlichting, H., McGraw-Hill, 1960, pg. 595.

It was learned, during calibration tests, that excessive lengths of loose signal cable gave rise to spurious DC signals, when the cable was flexed. Presumably, these effects resulted from triboelectric charge separation in the cable dielectric insulation. If the cable was motionless, no such signals were generated. To minimize such effects, an unavoidable concommitant of the impulsive motion experienced in calibration runs, the shortest practical length of cable was used.

The final cable length, therefore, reflects a calibration problem. In a final field design, where the signal cable can be housed rigidly, there is no indication of limitation on length.

2. Ion Anemometer Wake

Consider the wake of the α source. Spherical in form and of 1 cm diameter, the appropriate Re at 1 MPH is about 320. Lacking 3D empirical data in this Re region, use is made of the general conversion expression relating 2D to 3D wakes. The 3D wake* velocity decrement $\Delta V = K/(\text{distance})^{2/3}$ diminishes more rapidly with distance than the 2D wake (see 2D cylinder expression, prior page). Assuming a 5 percent velocity decrement to be acceptable, the appropriate distance downstream sufficient to regain 95 percent of free stream velocity is 2.3 sphere diameters, or less than one inch. The source was generally placed at a greater distance from the field voltage electrodes in the course of the calibration experiments; thus the source was not permitted to "shadow" the field voltage electrodes. However, those ions in the immediate vicinity of the source may be expected to experience an aerodynamic disturbance; trajectory computations of this disturbance were not performed.

Grid wake characteristics were not analyzed; no accurate 3D expression is known to the authors.

---

* "Boundary Layer Theory," Schlichting, H., McGraw-Hill, 1960, pg. 604.

4. Calibration Technique

A. Background

The calibration of wind measuring devices is a classic problem in instrumentation. There are but two basic choices; moving the instrument through stagnant air or moving the air through the instrument. Into the first category fall whirling arms and sleds, wind tunnels make up the second group.

Whirling arms date from the time of Langley, and perhaps earlier. The device to be tested is mounted on an arm capable of moving at a known tangential velocity within a stagnant atmosphere. The advantages are those of extreme simplicity. However, there are major sources of difficulty: 1) Electrical contact with the device is difficult to maintain. 2) The passage of the arm through the air produces a sufficient disturbance so that wake crossing problems arise. 3) The "stagnant" air slowly begins to rotate as viscous effects become prominent.

While there are procedures available to offset these problems, some years of experience with whirling arms in connection with the calibration of hot wire anemometers resulted in a negative decision. The key difficulties foreseen were: 1) Carrying off the low currents realized (approximately 10^{-9} amp). Our experience has been that the best of "brush" pickups (mercury bath) grow troublesome at current values less than 10^{-7}. 2) Shielding the arm path from external fields so as to perform certain environmental tests.

A low speed tunnel, once calibrated and tested for uniformity of velocity profile, is an admirable test facility. In view of the ready local availability (N.Y.U. Low Speed Tunnel) of a calibrated (smoke puffs) tunnel, a number of preliminary tests were conducted to check practicality. It was

found on windy days the open circuit (i.e., fresh air is constantly drawn in; there is no recirculation) nature of the tunnel produced serious aberrations in the tunnel calibration, in the velocity range of interest. This condition was found unacceptable. Consequently but few data collecting runs were made in the N.Y.U. Low Speed Tunnel. Nonetheless, those few runs were useful, principally in offering an extended velocity range as compared to the sled facility, finally chosen as optimum.

Certain runs were conducted in a separate wind tunnel, referred to as the insect tunnel. The latter is an open throat, open circuit tunnel. While lending itself to simple yaw testing, inadequate velocity regulation precluded output versus velocity testing. Therefore but little use was made of the insect tunnel facility; usage restricted to yaw testing.

Sled calibration devices, in which the instrument is transported along a track within a closed box containing stagnant air, are seldom employed. The primary difficulty is one of great track length required for a high velocity run. Other difficulties include the considerable mechanical complexity involved in clutching (in and out) the sled, recycling the sled to its starting position, absorbing the sled acceleration without damage to the instrument, paying out wires to the instrument and varying the sled speed. Sled advantages are largely those of simply determined velocity and freedom from concern over velocity profile. At the vanishingly small velocities of interest, track length and mechanical complexity problems are tractable. Consequently, it was decided to construct a sled calibration facility.

B. Sled Concept (See Figure 4-1)

The sled calibration device consists of a box, all sides of which are closed. A track, bolted to the floor of the box, contains a slide fitted to

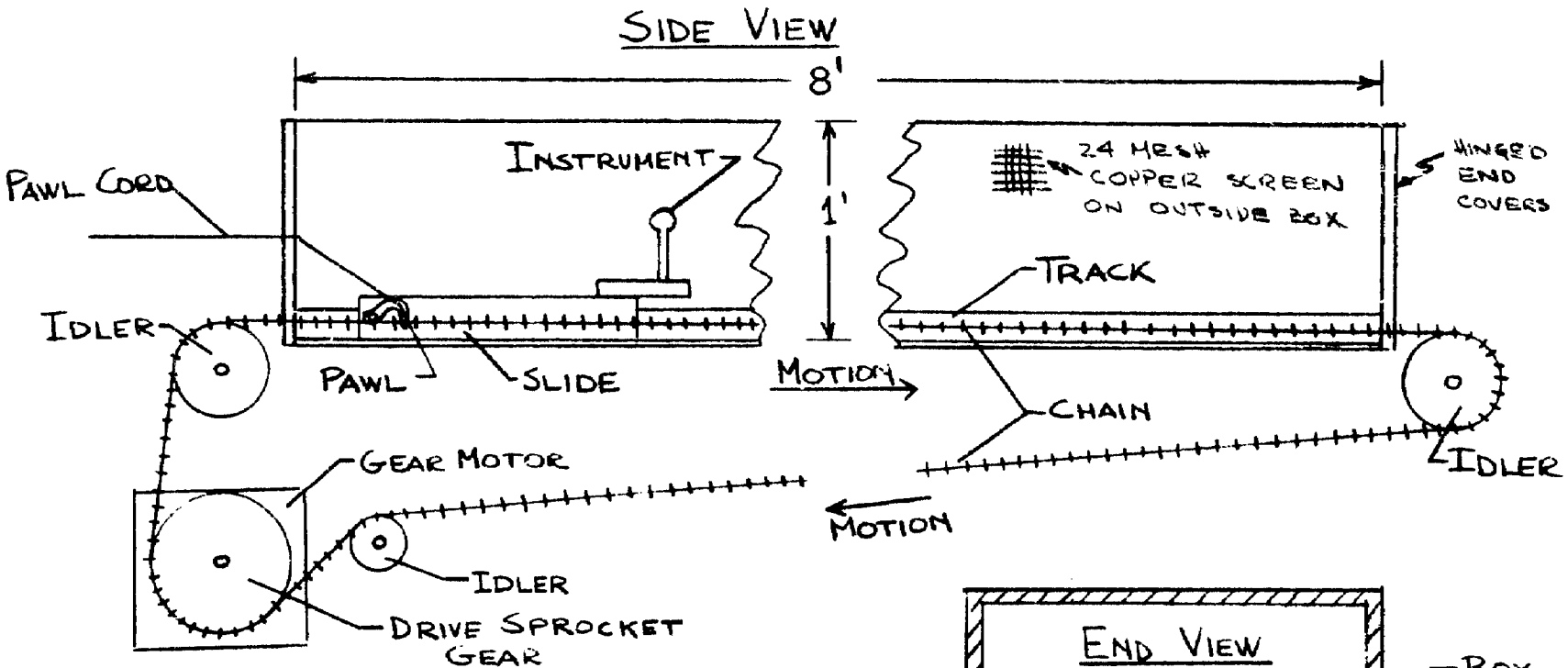

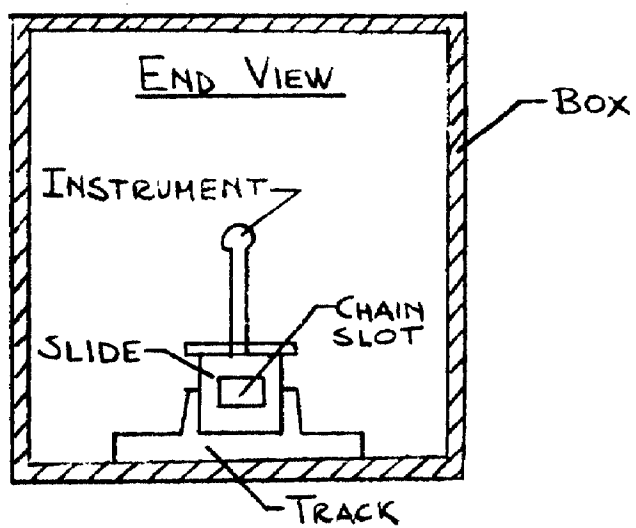

SLED TEST FACILITY SCHEMATIC

MECHANICAL ARRANGEMENT

FIG NO 4-1

to the track. The instrument under test is mounted to the slide. A metal chain in the form of an endless belt passes through the slide, the track, and through small holes in the box ends. Passing over idler pulleys the chain leads to a heavy duty variable speed gear-motor equipped with a sprocket drive wheel.

In operation, the gear motor-chain combination is brought to the desired speed, with the slide stationary. A pawl (hook) mounted in the slide, lowered into the moving chain, propelled the slide. As the inertia of the slide is small and the momentum of the chain drive is large, the sled (and instrument) are brought to chain velocity impulsively with little time lag. The box length is such that between roughly 2 and 10 seconds (depending on the velocity) are available at steady state velocity conditions, in which to take readings. For a typical slide-gear motor setting calibration see Figure 4-2. An automatic device releases the pawl from the track at the end of the run. The slide is then returned manually to the starting position. To prevent wake crossing, a delay of one minute between runs is used to permit the wake to attenuate. Velocity determination is through stop watch measurements of the elapsed time for a complete chain circuit transit.

C. Sled Test Facility Details

The gear motor drive is a Varidrive (U.S.Motors) 1/4 HP with a minimum speed of 11 RPM and a maximum speed of 113 RPM. The chain is No. 2 Ladder Chain (Boston Gear) passing over an 80 tooth drive sprocket gear and a set of three idler sprocket gears.

The box is 8 ft. long and 1 ft. on a side. Hinged ends are latched to complete the closure. Construction is of shellaced 3/4 inch waterproof plywood. Three large hand holes on the top face permit instrument adjustment.

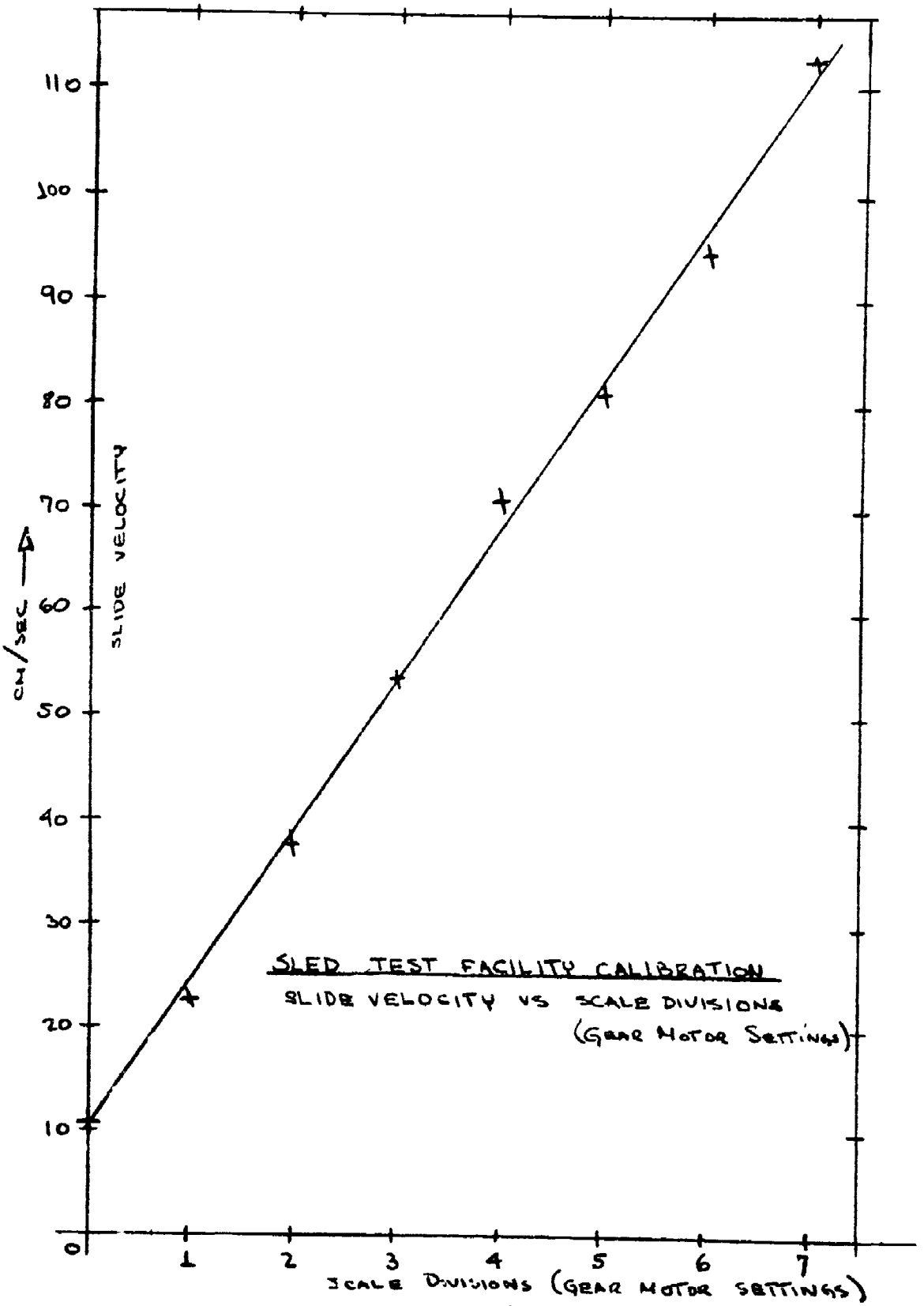
110
100
90
80
70
60
50
40
30
20
10
0
CM/SEC →
SLIDE VELOCITY
1
2
3
4
5
6
7
SCALE DIVISIONS (GEAR MOTOR SETTINGS)
SLED TEST FACILITY CALIBRATION
SLIDE VELOCITY VS SCALE DIVISIONS
(GEAR MOTOR SETTINGS)

FIG. NO. 4-2

The hand holes are covered, in operation, with flush plates screwed tight.

The track is an 8 ft. aluminum extrusion of channel form. The slide is fashioned of cloth based phenolic and finished to a sliding fit in the channel. No lubricant is used. The chain passes through the center of both channel and slide. A slot milled the length of the slide, on center, permits chain passage.

The pawl is spring loaded in the engaged position, i.e., unless consciously restrained by means of tension applied to a cord leading out of the box through an end plate, the pawl is engaged. In starting up the motor drive, or whenever the sliding action is not desired, it is necessary to pull on the pawl cord. When the slide reaches the end of its run, a large knot on the pawl cord is caught by a smaller hole in the end plate. As the slide continues to move tension is applied to the pawl cord. When sufficient tension exists to overcome the initial pawl preloading, the pawl is withdrawn from the chain and the slide stops. To return the slide to its initial position, the pawl cord is "reeled in" moving the slide the full length of the box against the motion of the chain. It is not necessary to stop the chain at any time.

Wiring to the instrument under test consists of three leads; two high voltage leads and a single output wire. The high voltage leads are attached to a rotary brush type retracting spool mounted within the box. The retracting device (commercial) is of the type used in automotive repair work. Wire payout with the device, modified slightly to eliminate stops and latching detents, is fully automatic as is retraction. In months of testing, no snarl has ever developed. The output wire is carried through the same exit hole as the pawl cord. Permitted to drape loosely, the output wire is handled

simultaneously with the pawl cord in terms of payout and retraction.

The box is shielded with 24 mesh (opening .028 inch) copper screen arranged to cover the entire exterior surface area. In locations where frequent openings (hand holes) make screen continuity difficult, brass plates are employed to assure both thorough shielding and good screen contact. The shield is joined to ground in all of the tests reported in this work, unless otherwise noted.

D. Angled Flow Tests

The desired response of the anemometer with respect to angled flow, (i.e., off-axis), is a reading of the directional cosine vector. As the anemometer has but a single axis of sensitivity, labelled the X-axis, only the X component should be discerned by an ideal instrument. In practice, however, the spatial asymmetry of the devices coupled with aerodynamic blockage inherent in any real instrument produced concern over the true response to angled flow. Consequently a series of tests have been conducted to gauge the extent of departure from a cosine response.

Such tests employ a means of varying the angular attitude of the anemometer with respect to the oncoming wind. Within the sled facility, a series of elbows were so placed as to permit angular testing through the angular ranges shown in Figure 4-3. Coordinate labelling taken from conventional aerodynamic notation is as follows. The X-axis is the main longitudinal axis of the instrument. The Y-axis is the horizontal axis perpendicular to the X-axis and the vertical axis. The Z-axis is the vertical axis. A vector within the X-Y plane maintains an angle of yaw, β, with respect to the X-axis. A vector within the X-Z plane maintains an angle of pitch, α, with respect to X-axis. A vector in the Z-Y plane maintains an angle of roll, ϕ, with respect to the Y-axis.

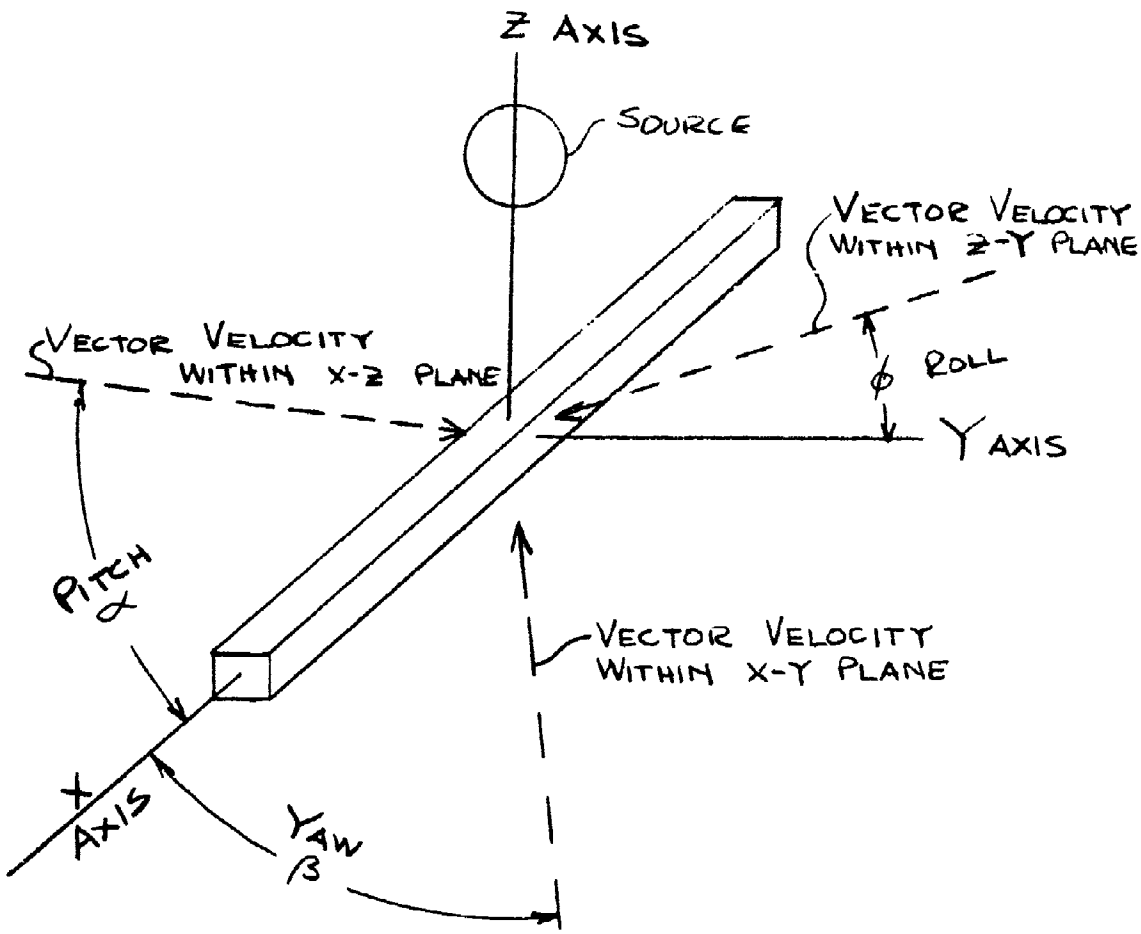

ANGLED FLOW
AXES CONVENTIONS

FIG NO 4-3

5. Experimental Results

A. Final Configuration

The final model ion anemometer was developed over some months of design modified by much cut and try testing. It is not represented as an ultimate solution, but rather the best design obtainable within a limited program.

The design configuration, shown in Figures 5-1 and 5-2, consists of a spherical radioactive source (less than 1 millicurie of Polonium 210) mounted on a stem above a polystyrene base. A fine-mesh copper screen, rectangular in outline, is fixed on the stem just below the α particle source. This screen, aligned with the device's sensitive axis, serves as the center probe. At right angles to the probe screen and symmetrically placed some short distance out from each edge of the probe, are two electrodes in the form of coarse rectangular screens which act as the high potential field electrodes. This geometry, of all the configurations tested, was found to give the best results in terms of linearity, cosine law angular response, and no saturation over the wind velocity range of interest.

In use, the two outer electrodes are connected to the positive and negative terminals of an adjustable high voltage supply, typically operated at 2000 volts. The center probe electrode is connected through a current measuring circuit to a grounded tap on a potentiometer across the high voltage supply.

By adjusting this potentiometer tap, the relative and negative voltages of the outer electrodes can be altered with respect to the center probe. In effect, the field electrode voltages can be differentially changed so as to adjust electrical balance until the probe current reads zero indicating balance.

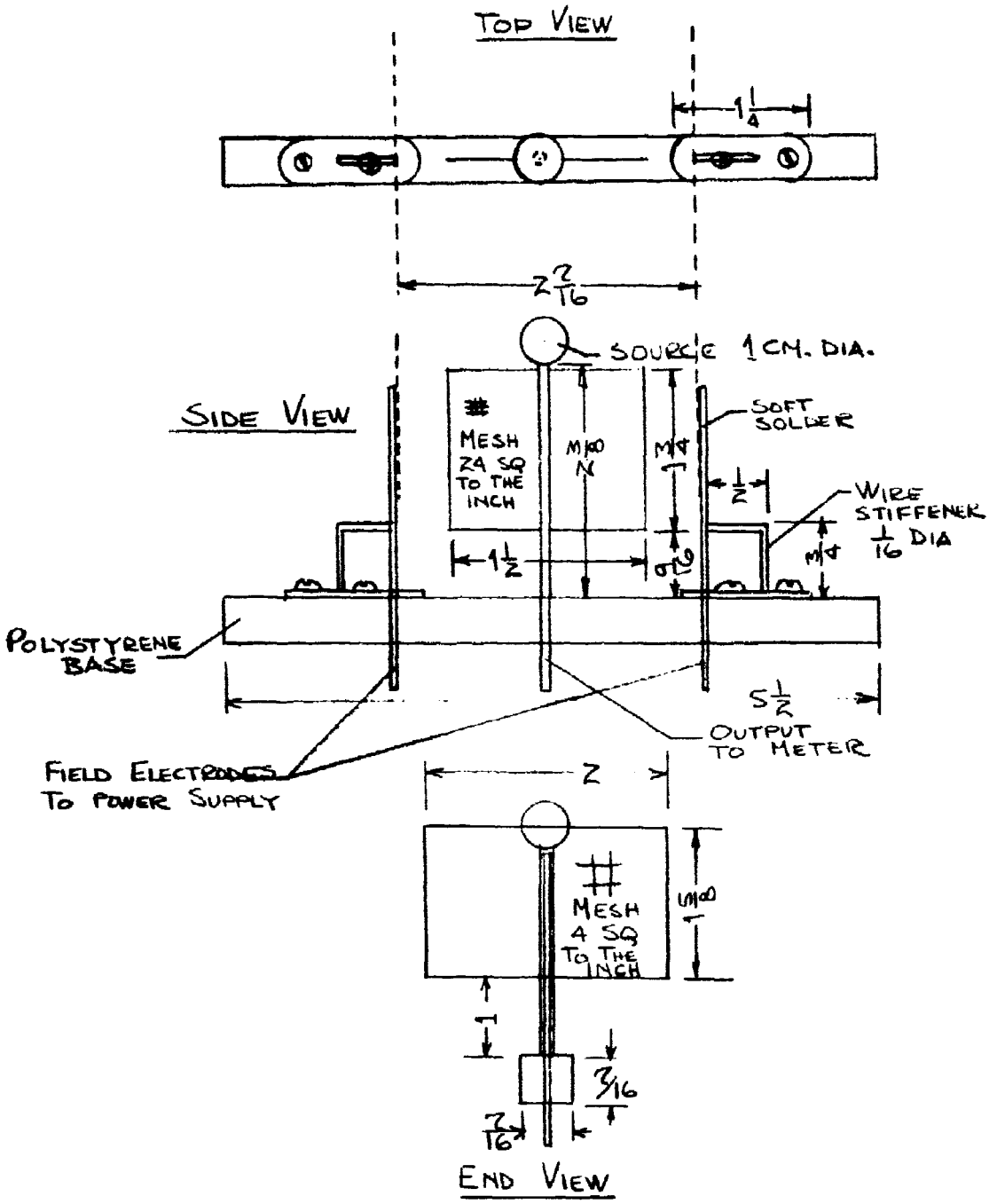

FINAL MODEL - ION ANEMOMETER

MECHANICAL ARRANGEMENT — NOT TO SCALE

FIGURE NO 5-1

FINAL MODEL - BASE SUPPORT & MECHANICAL ARRANGEMENT

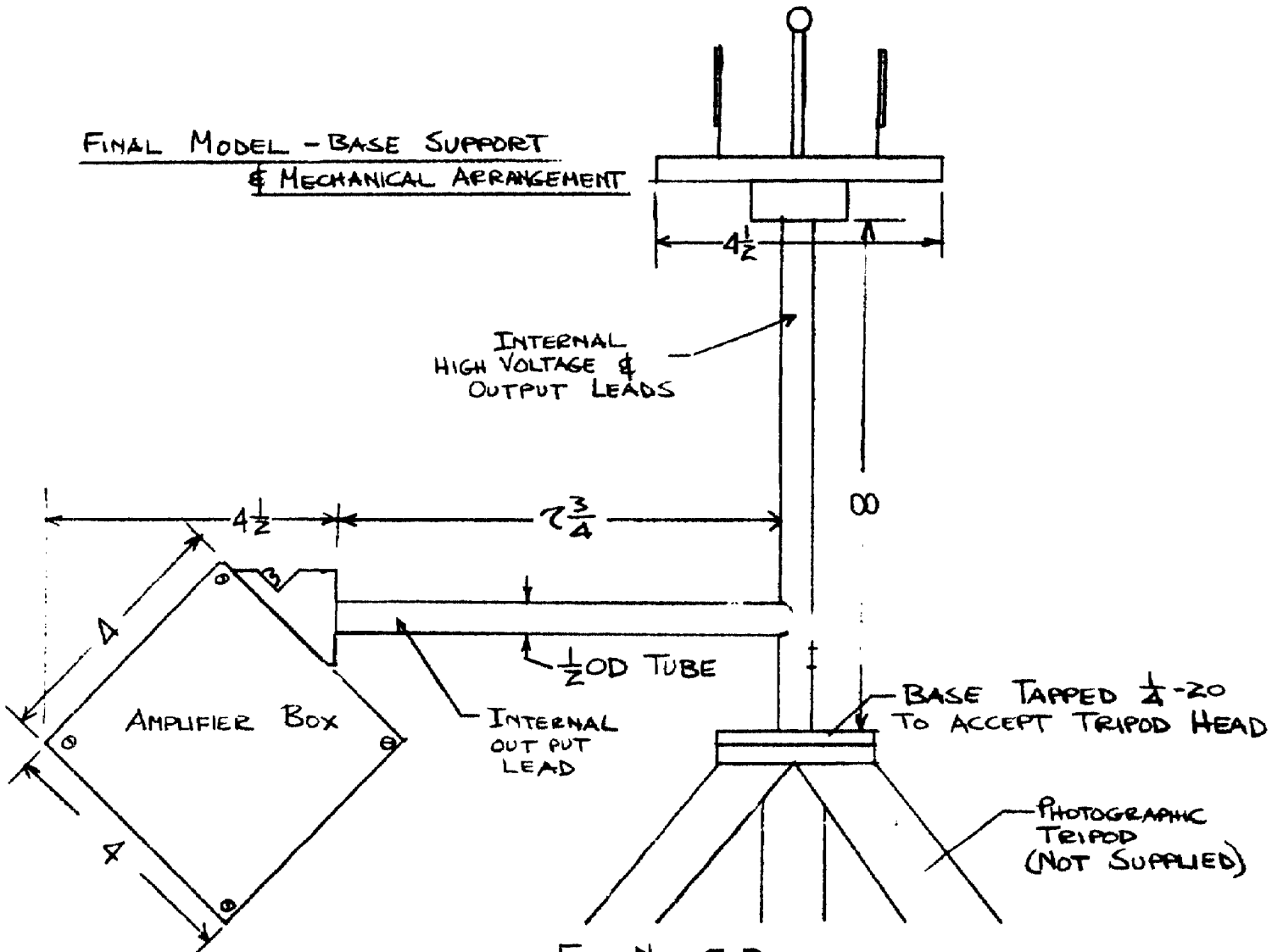

FIG NO 5-2

B. Principles of Operation

In operation, equal numbers of positive and negative ions are created in the region between the two outer field electrodes by the passage of the alpha particles through the air. These ions are continuously swept up by the electric fields existing between the two high voltage field electrodes. Positive ions are collected by the negatively charged electrode and negative ions by the positive electrode. The source of ionizing radiation is centered between the electrodes and thus produces an approximately symmetrical cloud of ion pairs for collection by the electrodes.

The electrical potentials of the two collectors are initially equal and opposite with respect to the center probe which is electrically grounded through a current measuring electrometer circuit. In the absence of any wind and with perfect geometric symmetry of source, probe and collectors, equal numbers of positive and negative ons are collected per unit time by each outer collector electrode. Under these circumstances, the currents in each collector are equal and opposite and zero net current flows to the source-probe which may be considered to be a voltage probe ("Langmuir probe") immersed within the ion space charge cloud.

A small unbalance current will flow to the probe if it is located inside the ion space charge cloud at a point whose relative potential differs from that of the balancing potentiometer tap to which the probe is returned. This unbalance current will be positive or negative, depending on which side of the null point the potentiometer tap has been placed.

Similarly, if the source-probe is physically displaced from the geometric center of the two collector electrodes while its electrical return is still midway between the collector potentials, then it will also draw current from the ion space charge cloud.

A valid analogy to this device, then, is the following simple potentiometer circuit:

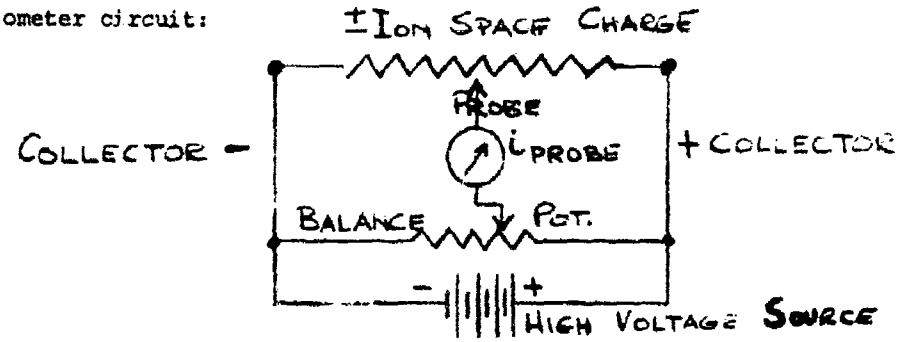

Thus, zero probe current implies that the voltage difference between its active end immersed inside the ion cloud and its electrical return to the balance potentiometer has been reduced to zero.

In the absence of wind, and with the probe physically centered between the collector electrodes, the balance potentiometer is set so as to null the probe current. Thereafter, any component of wind along the sensitive axis (between the outer electrodes and through the probe) will alter the distribution of ions so as to change the potential of the probe. This unbalance is indicated by a current flow in the probe's current measuring circuit, positive current resulting from wind towards the positive collector and negative current from an opposite wind.

The original concept for this ion anemometer envisioned its use as a continuously nulled or balanced instrument. It was expected that if the probe electrode's return tap on the potentiometer were continuously adjusted so as to null the unbalance current, probe offset voltage (from the null position at zero wind) would be a linear measure of wind. Of course, for actual field use in winds of variable velocity, the manual nulling potentiometer would have had to be replaced by a continuously nulling electronic servo system.

This mode of operation results in an output signal, namely the probe error voltage or offset with wind from the zero wind point on the balancing

potentiometer, which measures in the hundred volts. However, it has been found, invariably, that the calibration curves given by the nulling technique are neither more nor less linear than those resulting from direct readings of probe unbalanced current. In other words, the unbalance current itself is exactly as valid a measure of instantaneous wind as the probe offset voltage added to rebalance probe current to zero.

Admittedly, the probe unbalance current is typically small (10^{-9} amperes), but it must be amplified anyway as an error signal in trying to null the instrument by the use of the balancing potentiometer. Furthermore, modern solid state operational amplifiers used as current-to-voltage converters, can convert such currents to output signals of the order of a volt at low impedance in a stable, linear and accurate fashion.

Accordingly, the instrument is designed to supply a low voltage output signal which is a measure of the probe's unbalance current, and the manual balancing potentiometer (helipot) is used only for nulling at zero wind and for checking calibration, as will be discussed below in Section 5.F.

C. Instrument Operation

As the experimental data and final calibration runs show, the unbalance current is a linear measure of the on-axis wind component. The measured current is of the order of magnitude of 10^{-9} amperes, for the particular radioactive source and source placement used in the present device. This level of DC current is accurately and easily measureable by means of present day commercial differential operational amplifiers used as current-to-voltage converters (electrometers). The circuit used a Philbrick SP2A solid-state varactor-bridge stabilized, differential amplifier with an external feedback resistor of 10^{9} ohms. Its output is given by $E_o = - i \times 10^{9}$ volts, so that an input current of

10^{-9} amperes produces an output signal of 1 volt.

In use, the anemometer and signal amplifier supply voltages are turned on, and with the sensing head screened from any ambient air currents by means of a hood, the probe's unbalance current is nulled by adjusting a 10-turn helipot potentiometer. Under these conditions, - namely, full operation at zero wind, probe current nulled, - the instrument is zeroed and ready for normal use when the wind screen or hood has been removed.

Extensive experience with many configurations of the device has shown that the zero is stable and that there is no need for frequent readjustment.

D. Experimental Results and Calibration Tests

The voltage signal versus velocity calibration curve is linear (see Figure 5-3) and repeatable. In Figure 5-3, two calibration lines are shown. They depict the outputs of the instrument when equipped with two radioactive alpha particle sources of different strengths. A discussion of the effects of ambient temperature on the calibration curves is presented in Section 5-E below.

Figures 5-4 and 5-5 depict the measured response of the instrument, at a fixed wind velocity, to variations in the angles of pitch and yaw, respectively. Both sets of experimental points closely approximate the ideal normalized cosine curve at the air velocity employed.

Figure 5-6 shows the instrument output versus the angle of roll at an air velocity of 52.0 cm/sec. The experimentally observed points seem to be randomly scattered with a maximum output signal of 0.06 volts, approximately 10 percent of the signal obtained for this air velocity on-axis as shown in Figure 5-3. An ideal result would be zero output for all values of roll angle.

FINAL MODEL ANEMOMETER PERFORMANCE

VOLTAGE OUTPUT VS. AIR VELOCITY
FIELD VOLTAGE : 2000 V.

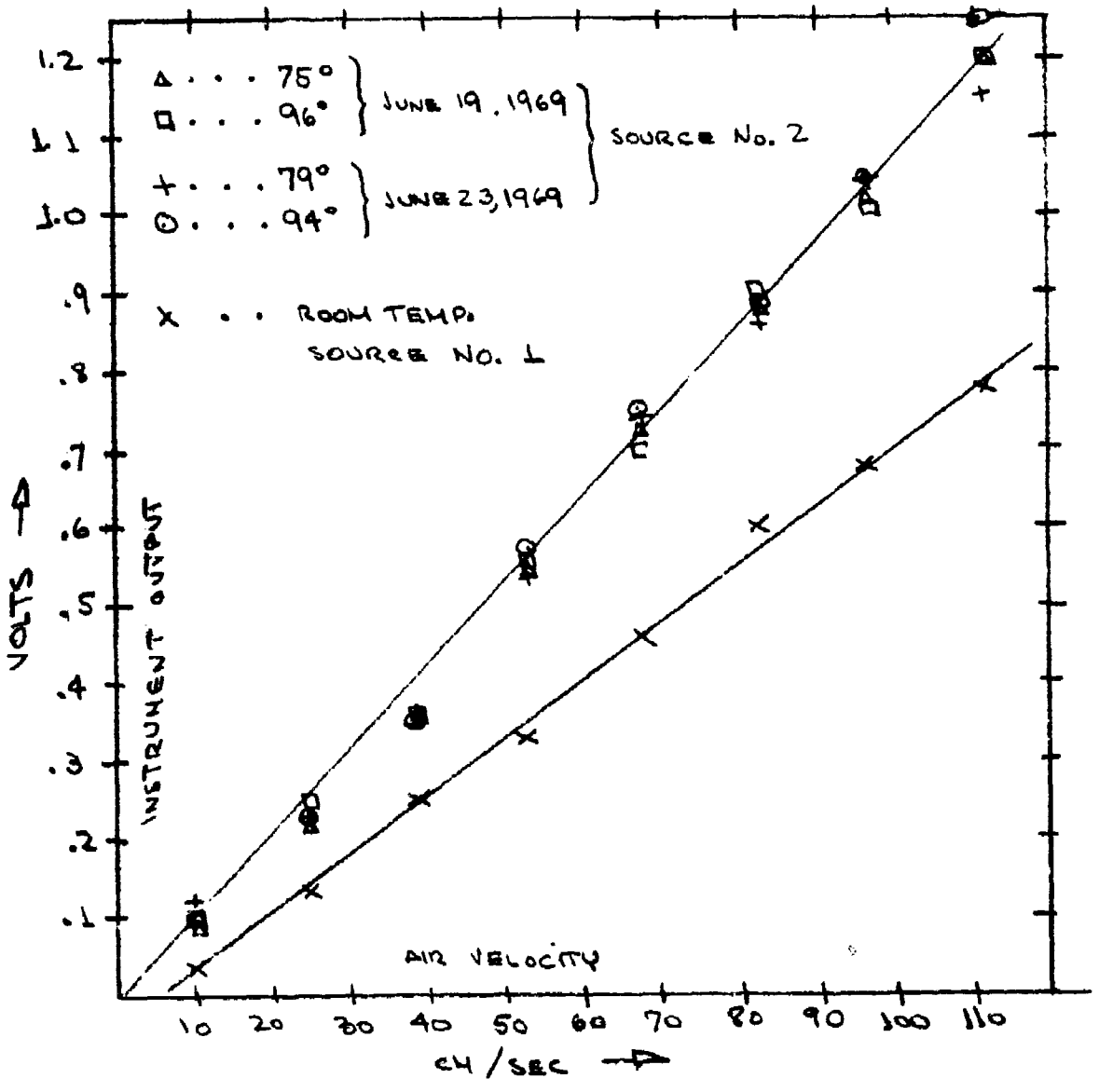

FIGURE NO. 5-3

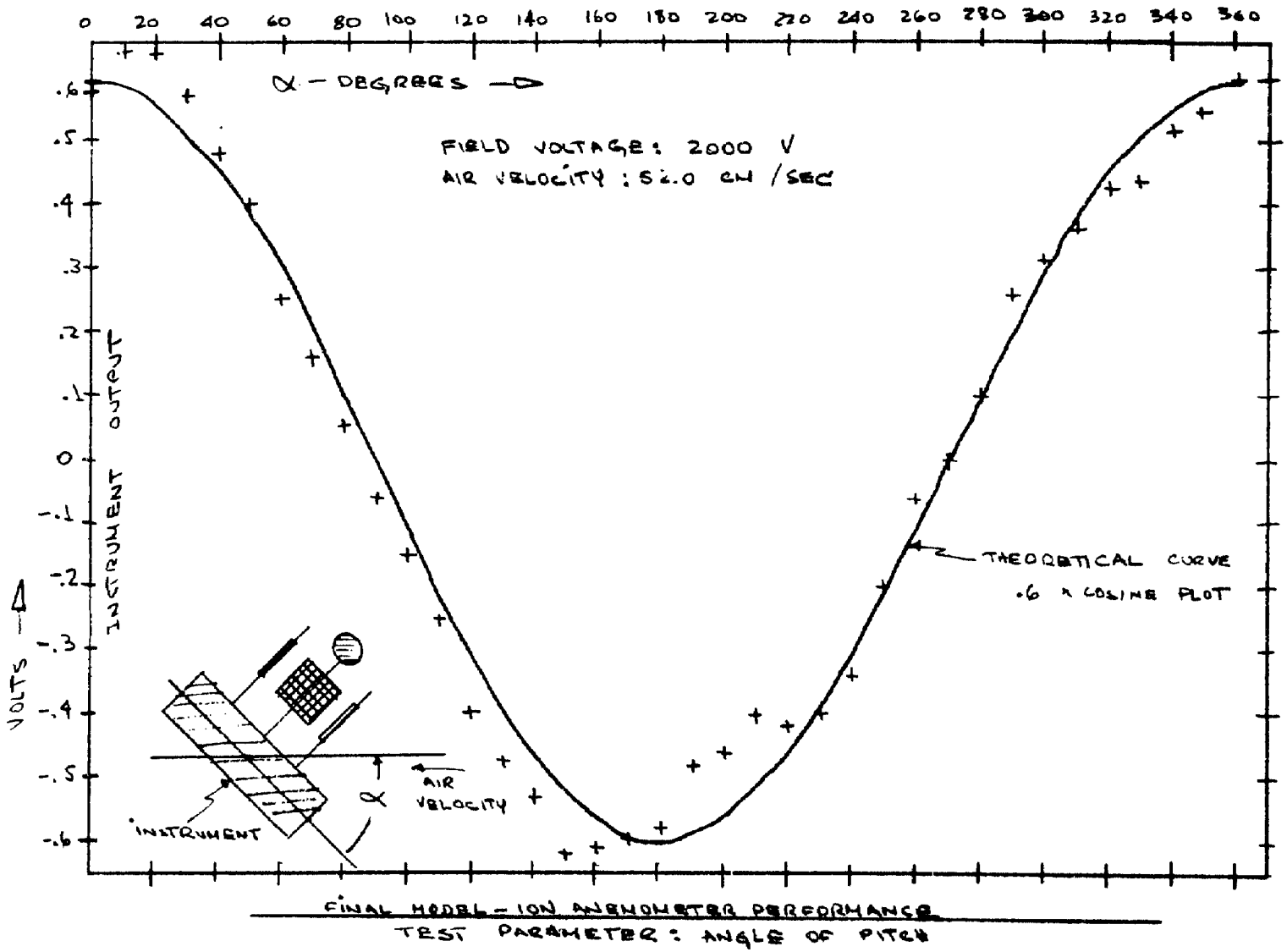

FINAL MODEL – ION ANEMOMETER PERFORMANCE

TEST PARAMETER: ANGLE OF PITCH

FIGURE NO. 5-4

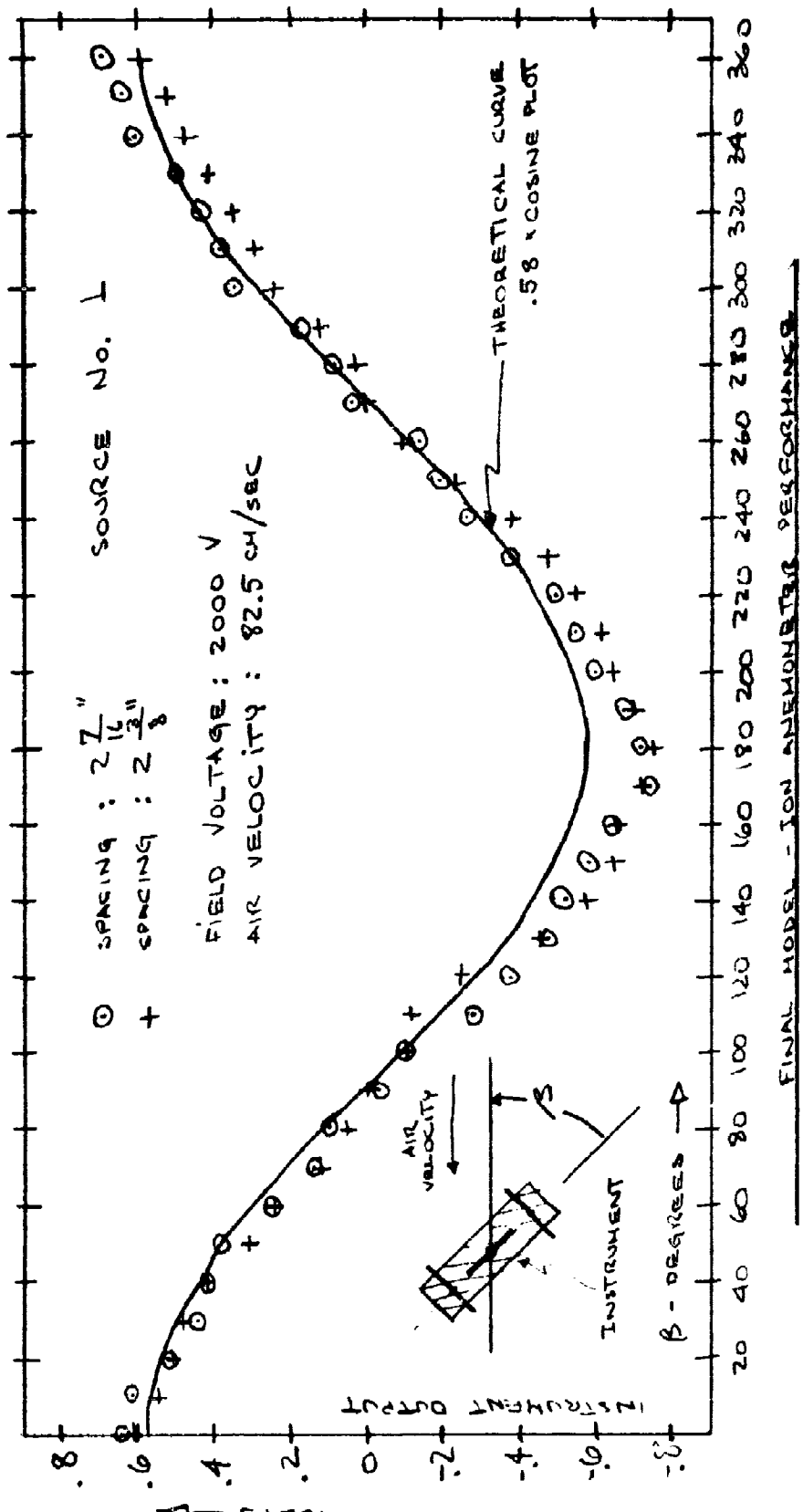
SOURCE No. 1
SPACING : 2 7/16"
SPACING : 2 3/8"
FIELD VOLTAGE : 2000 V
AIR VELOCITY : 82.5 cm/sec
THEORETICAL CURVE
.58 x COSINE PLOT
INSTRUMENT OUTPUT
VOLTS
B - DEGREES
AIR VELOCITY
INSTRUMENT
FINAL MODEL - ION ANEMOMETER RESPONSE
TEST PARAMETER : ANGLE OF YAW

Fig. No. 5-5

FIELD VOLTAGE : 2000 V

AIR VELOCITY : 52.0 CM/SEC.

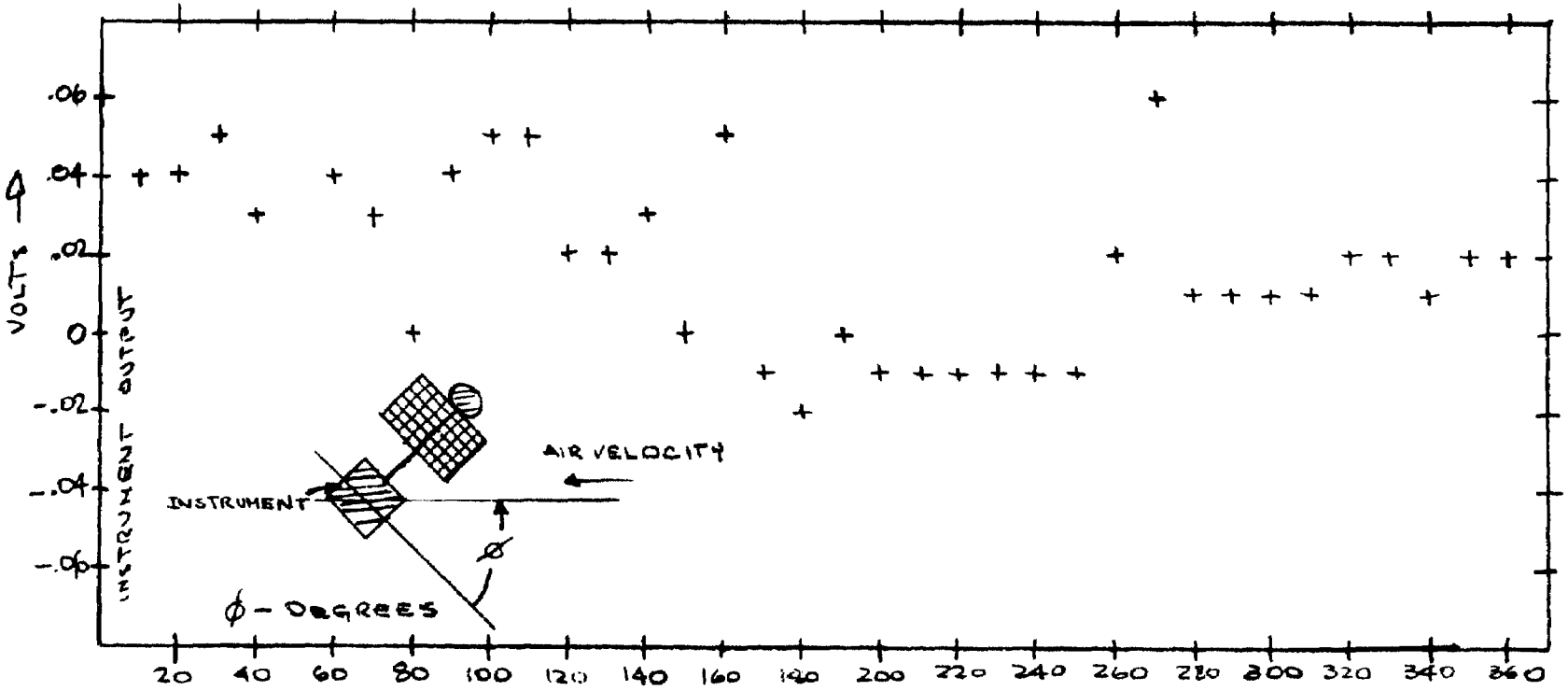

FINAL MODEL - ION ANEMOMETER PERFORMANCE

TEST PARAMETER : ANGLE OF ROLL

Fig. No. 5-6

E. Environmental Factors

1. External Electrostatic Fields

In the great majority of experimental tests conducted with the ion anemometer, a copper screen connected to ground and completely surrounding the sled test facility was employed to shield the instrument from external electrostatic fields. Limited testing with either the ground lead disconnected (sled test), or the screening entirely removed (insect tunnel), produced the following results.

Varying the local field intensity by such external means as arm waving within inches of the device behind a paper aerodynamic shield, has a definite effect on instrument output. The response is large (on the order of 50 percent full scale) for a changing external field, and small (approximately 5 percent full scale) for a static external field. When the source of the external field is withdrawn to approximately three feet from the instrument, little or no effect is produced by either static or dynamic fields.

Instrument configuration and field voltage are significant in determining the effect of external fields. Configurations with high interelectrode fields are not greatly affected, whereas those with low interelectrode fields are. It is our view that the final configuration will operate properly, unshielded, even in the proximity of sizeable static external fields. Dynamically changing external fields, such as might be produced by a charged and waving tree branch, should be separated from the device by a distance of at least three feet.

2. Humidity and Rain

To test the ability of the instrument to accept conditions of high humidity and rain, a cup of water on a hot plate was boiled off within the sled

test chamber while the instrument was operating at a zero wind condition. The resulting condensation filmed over the instrument (final configuration) with water. Useful readings were not obtained under these conditions; it iw believed that the alpha source was completely attenuated by the water coating. However, the instrument evidenced no arcing or other signs of damage. It proved necessary to raise the field voltage from the standard 2000 volts to approximately 5000 volts to initiate arcing. Upon simple air drying (the latched ends of the sled test facility were opened to permit ventilation for ten minutes, then closed), the instrument worked without requiring any readjustment and without any change of calibration.

3. Radioactive Source Decay and Contamination

During the course of the months of test work the alpha particle sources experienced a normal decay in strength, in conformity with the 0.3 year half-life of Polonium 210. In addition, despite care in handling the sources so as to minimize contact with the active surface, contamination inevitably resulted from the deposition of active components of the sled test chamber atmosphere such as oil vapor and cigarette smoke. An important practical question thus arises: To what extent are the instrument's performance characteristics influenced by source decay and/or surface contamination?

Measurements of the source intensity for each of the two spherical sources (1 cm. diameter) were taken after approximately eight months of active test work and thirteen months after original manufacture. The data given in Figure 5-7 were obtained with a standard alpha particle radiation intensity meter placed so that the sensing element was approximately 7/8 inch from the surface of the spherical source and aimed at the sphere's "equator." By affixing the source stalk in a bearing mounted collet, the source could be rotated

about the stalk axis and manually positioned at 10 degree increments of longitude.

The sources display a significant angular assymetry and a significant difference in average level of output. We are uncertain of the cause of such intensity differences, because, unfortunately, no such intensity readings were taken when the sources were first received. Thus it is unclear whether the supposed symmetrical and equal strength sources were poorly manufactured originally or decayed to the observed level of non-uniformity through wear and/or deposition. Cleaning operations were confined to spraying with a commercial Freon degreasing agent with no subsequent rubbing or wiping. It is possible that improved cleaning techniques might aid in maintaining source uniformity.

The lack of source symmetry is believed responsible for certain difficulties encountered during calibration. In particular, there has consistently been a difference (approximately 9 percent) in instrument output at yaw angles of 0° and 180° for all air velocities. Such a difference, which persisted despite the most painstaking positioning of the device parts, can only reflect some lack of symmetry in the device. We believe that the source non-uniformity could account for the observed $0^{\circ} \neq 180^{\circ}$ inequality.

It has also been observed that different instrument sensitivities resulted from changing sources, i.e., the slope of the output signal versus velocity curve is different for an instrument altered in but one respect, - the exchange of one source for the other as shown in Figure 5-3. But as Figure 5-7 clearly demonstates, the mean radial radiation intensity is different for each source, which could account for the observed differences in sensitivity.

Another question which arose during the testing of the final instrument

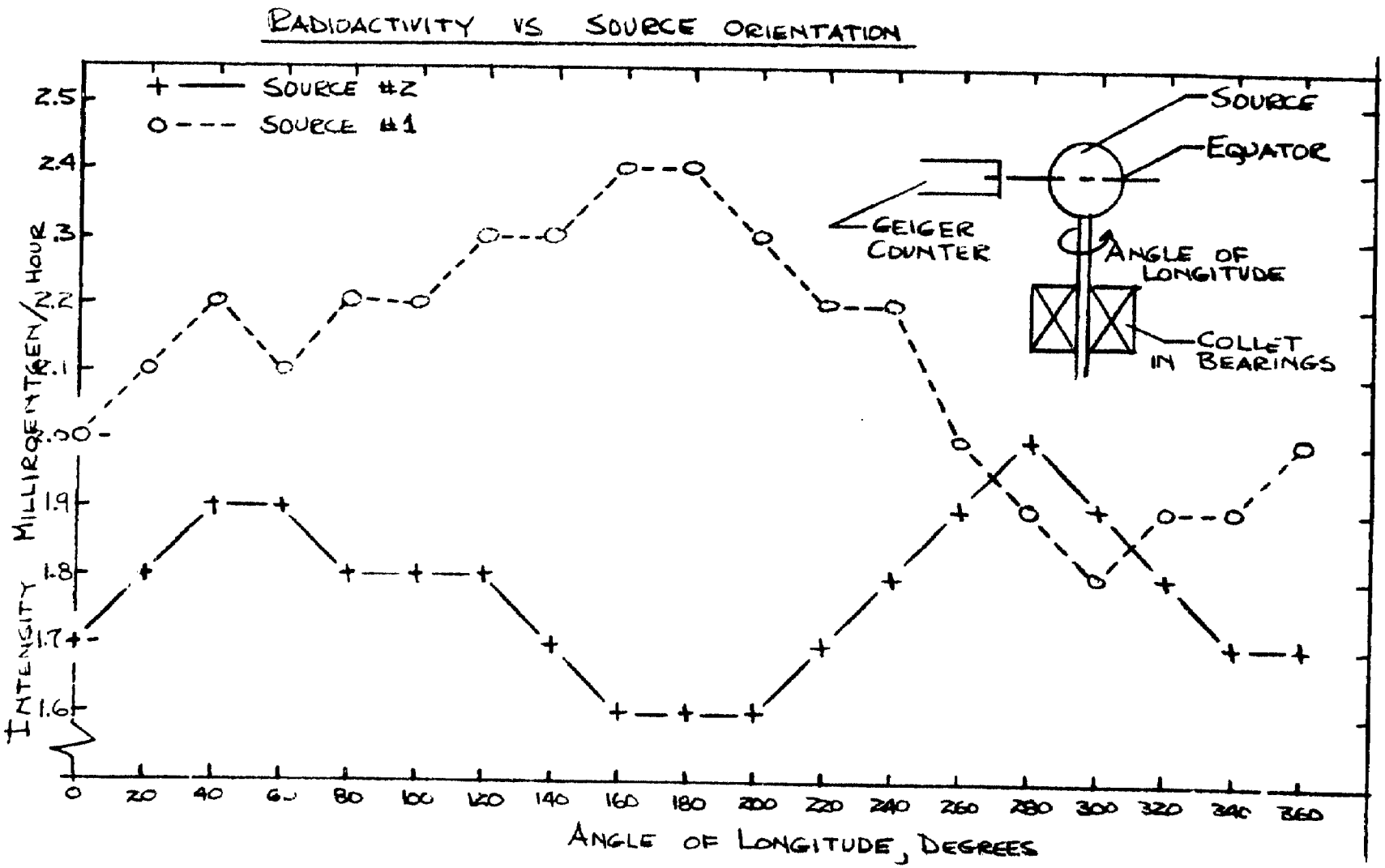
RADIOACTIVITY VS SOURCE ORIENTATION
SOURCE #2
SOURCE #1
SOURCE
EQUATOR
GEIGER COUNTER
ANGLE OF LONGITUDE
COLLET IN BEARINGS
INTENSITY MILLIROENTGEN/N HOUR
2.5
2.4
2.3
2.2
2.1
2.0
1.9
1.8
1.7
1.6
0
20
40
60
80
100
120
140
160
180
200
220
240
260
280
300
320
340
360
ANGLE OF LONGITUDE, DEGREES

FIG No 5-7

concerned the extent of ionization outside the two outer collector electrodes. It was felt that any such effect would detract from instrument performance. Therefore, measurements were made by pressing the sensing head of the radiation meter against the outer faces of the mesh collector electrode. The observed alpha particle count was approximately 20/min., or only twice the normal background count. It follows that all source alpha emission is contained within the space between the two outer electrodes.

4. Atmospheric Pressure and Temperature Effects

Since ion mobility is known to be an inverse function of air density, tests were conducted to determine the degree of dependence. By means of an electric hot plate, the air within the closed sled test chamber was raised in temperature approximately 20° F, causing a density decrease of approximately 6.5 percent. Subsequent testing (at the elevated temperature) with one source produced an increase in output sensitivity with velocity of approximately 20.5 percent. A similar test applied to the other source (see Figure 5-3) showed no significant change. To explain these disparate results, it is suggested that ion mobility per se, over the range of temperature tested, is of less consequence than the effect of temperature on alpha particle transmissivity of source surface contaminants. In any event, no clear temperature-sensitivity trend emerged from these tests.

F. Self-Calibration Technique

In view of the difficulty in accurately calibrating a low speed anemometer and the fact that source strength decay will affect instrument sensitivity, it would be useful to have a means of checking and recalibrating the instrument in the field. In fact, self-calibration is perhaps an essential feature for this instrument since to the best of our knowledge, the only accurate

calibration test facility available is the sled test chamber described in this report.

Such a self-calibration procedure is discussed herein and some preliminary corroborative tests of the technique are described.

Consider a previously calibrated ion anemometer whose source has aged since the time of calibration. With the device set up in the field, the operator, desiring to check the instrument's calibration or sensitivity, places a hood over the device so as to insure zero wind. Then he deliberately offsets the balancing potentiometer from the true null by a pre-determined increment. The effect is to produce a probe unbalance current and hence an output signal.

If the instrument is still "on calibration," the reading will correspond to a particular point on the original output-versus-wind velocity calibration curve. That is, the nulling potentiometer offset produces an output signal identical to that generated by placing the instrument in a known wind environment. In effect, this procedure can produce a simulated wind.

If the output signal resulting from the deliberate offset is lower than the nominal value expected, then the instrument is "off calibration" due to source decay or some other environmental factor. However, it is now a straightforward procedure to increase the gain of the signal current-to-voltage converter (operational amplifier) by varying the amplifier's feedback resistor ($V_{out} = - iR$) so as to produce the correct output signal. By this means, the instrument can be restored to its original calibration. Since the original calibration curve is linear, a "one point" readjustment as described above will suffice. The equivalence of the signal resulting from deliberate probe voltage offset and that from wind is evident from the following considerations:

observation has shown a consistent proportionality between the ion anemometer's probe unbalance signal current due to wind and the nulling potentiometer offset voltage required to balance out the signal current. In other words, one may plot unbalance signal versus velocity (as in Figure 5-3), or alternatively plot null pot voltage offset required to balance out signal current. The calibration curves resulting differ only in slope. Accordingly, one can reproduce the original calibration curve of probe output signal-versus-velocity by offsetting the balance potentiometer of appropriate increments.

To test this concept, an unusually intense source was prepared in the form of a cube, the vertical faces of which were coated with Polonium 210. Tested in the sled facility the output - velocity calibration curve of the instrument equipped with cube source demonstrated a slope approximately 750 times larger than that obtained with the conventional spherical source (an output, after amplification, of volts in contrast to the millivolts obtained with the spherical source). Using the technique described above, at zero wind, the nulling pot was offset one tenth of a full turn in the case of the spherical source and the resulting signal (4.6 millivolts) noted. The cube source was then inserted and amplifier gain reduced until the same signal was produced at the same pot offset. The resulting output-versus-velocity calibration curves indicated a difference in slope of 25 percent (first try) and 8 percent (second try) between cube and spherical sources. Thus, although restoration of calibration was not perfect, a considerable improvement was obtained; an improvement from an initial "error" of 75,000 percent to a final 8 percent. It is therefore our belief that in practice, this procedure will more than adequately correct for any changes in source strength. While untested, it is our belief

that such a procedure m also be used to compensate for environmental changes other than sour aging, changes such as slowly varying temperature and pressure factors.

G. Installation and Operation of the Ion Anemometer

The electrical connection diagram for using one of the anemometers at a time is shown in Figure 5-8. Two units can be used simultaneously on the power supplies shown, provided a second voltmeter is used (or a two channel recorder).

Each anemometer center probe is permanently wired by means of shielded cable to its attached operational amplifier input. The amplifier output signal lead, ground and the plus and minus fifteen volt amplifier power supply leads are all contained in a five wire shielded cable terminating in a five pin male connector.

The mating female connector has four emerging wires which are connected to power supplies and voltmeter as follows:

white to 1. High Voltate power supply ground
2. Operational Amplifier power supply (PR30) ground and chassis
3. Voltmeter (Hewlett Packard 919A) ground and minus input

red to + 15V terminal of PR 30

black to - 15V terminal of PR 30

green to + input of voltmeter

The anemometer collector electrodes are supplied with 2000 Volts DC by means of two insulated leads running directly from the base of the instrument to one of the two HV supplies. The chassis containing these two supplies also contains a small variac which permits the high voltage to be adjusted from zero to 5 kilovolts. Normal operation is at 2000 volts which is indicated by a

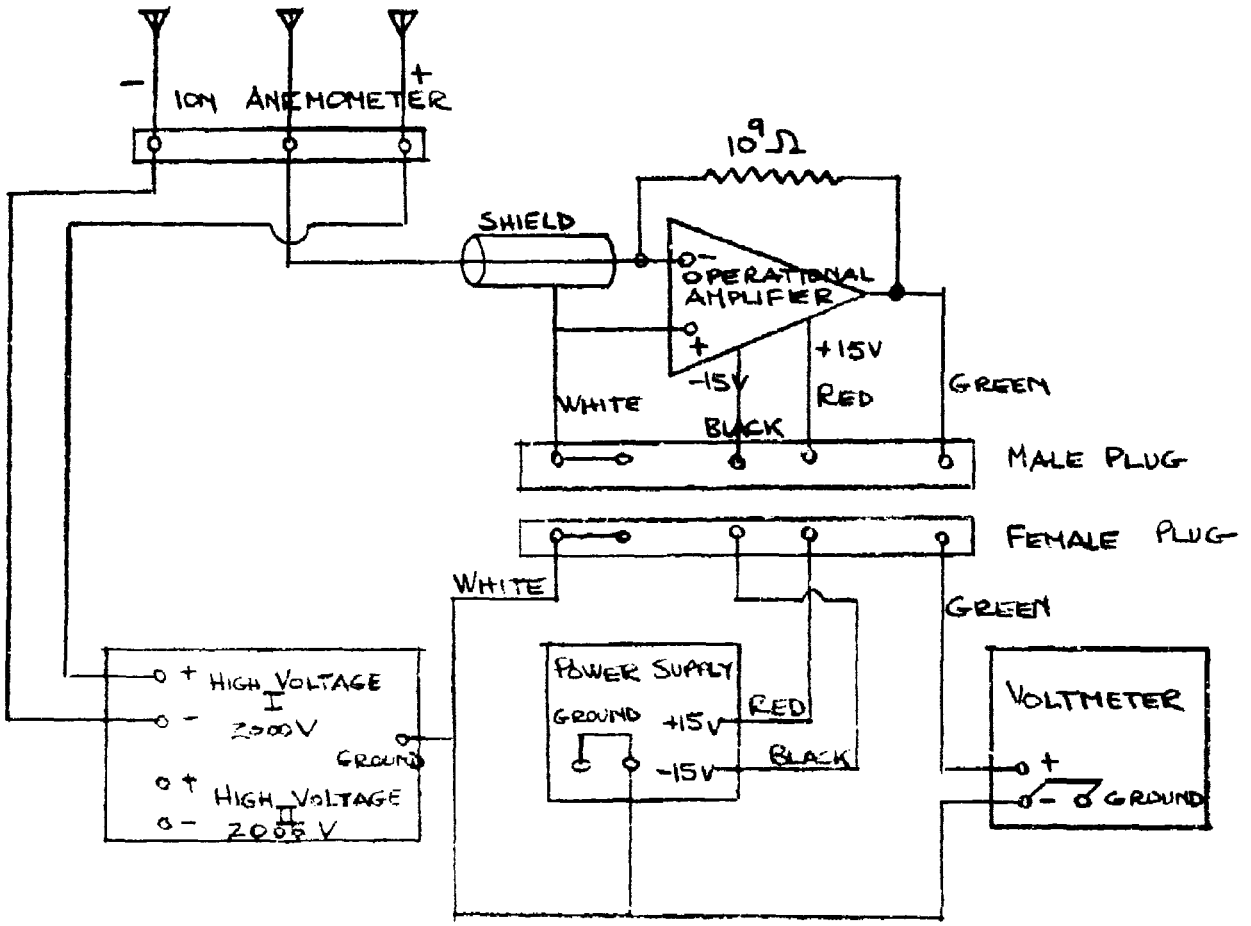

WIRING DIAGRAM

FIGURE NO 5-8

reading of 2 on a milliammeter on the front panel. These supplies were made variable for testing and development work, and might better be fixed for field use.

Two independent ten-turn helipots are used as the balancing potentiometers associated with each HV supply. A circuit diagram is shown in Figure 5-9. The PR 30 power supply is able to supply three amplifiers in parallel.

With all connectingwiring completed, the instrument is brought into full operation as follows:

1. Turn voltage control knobs of the high voltage power supplies to zero (fully counterclockwise);
2. Center the Zero-center voltmeter used to read output;
3. Turn on H.V. and PR 30 power supplies;
4. Turn up (cw) the voltage control knob of the high voltage power supply until meter #2 reads 2 ma or 2000 volts. If the same voltage reading does not appear on meter #1, then use the voltage adjust pot to equalize the two supplies;
5. With anemometer hooded (zero wind), the voltmeter must read zero output. If it does not, then adjust the nulling potentiometer (corresponding to the H.V. supply being used) until a zero output signal is obtained. Anemometer is now zeroed and ready for use as soon as hood is removed.

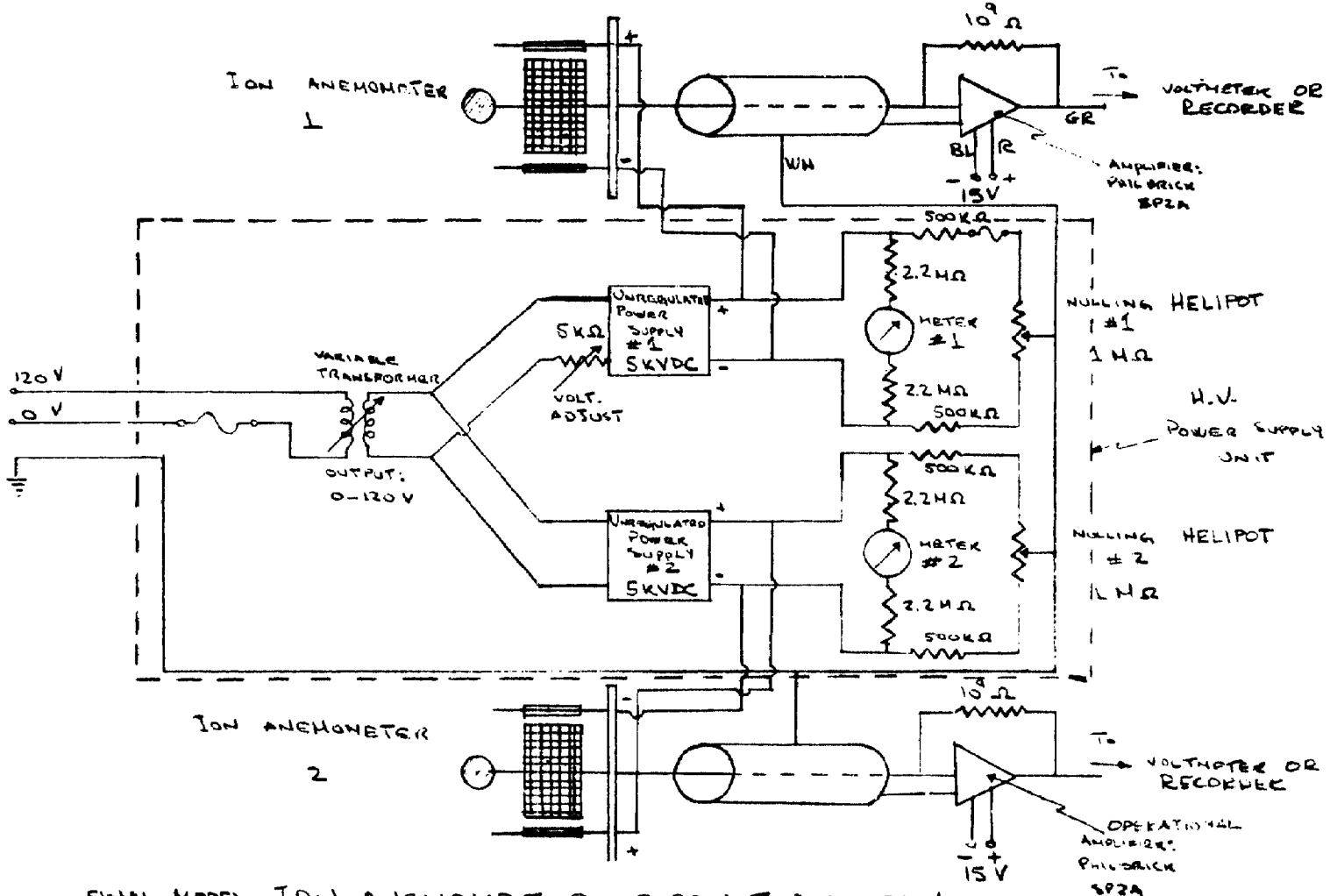

FINAL MODEL ION ANEMOMETER – CIRCUIT DIAGRAM

FIGURE NO. 5-9

6. Other Tested Configurations

A. Pin Electrode Configuration (See Figure 6-1)

The pin electrode configuration was so termed owing to the thin cylinders (pins) serving as outer electrodes. Mounted on a polystyrene base, the outer electrodes were arranged to offer adjustable spacing with respect to the center probe. The α source was placed above the center probe.

This configuration was found to offer the advantages of mechanical simplicity and a good cosine response to angled flow. However, difficulties in obtaining a linear velocity-output relationship at the higher end of the velocity scale (say, 120 cm/sec.) resulted in abandonment of the configuration.

Figure 6-2 depicts the instrument output (current; no amplification) under varied field voltages for a given outer electrode spacing. Note the tendency to "saturate" as the instrument velocity increases. For the electrode spacing employed (3-3/4 in.) the tendency to saturate was reduced by increasing the field voltage. However, this approach to linearization is subject to diminishing returns; examination of Figure 6-2 shows that successive incremental increases in field voltage produces a diminishing linearization effect.

When the electrode spacing is reduced (Figure 6-3) apparent linearity of the velocity-output curve is obtained (note 1-3/4 in. spacing curve). However, testing this arrangement at higher velocities (Figure 6-5) within the N.Y.U. Low Speed Tunnel indicated the undesirable saturation characteristic to persist.

Yaw tests of the pin electrode configuration, in which the response

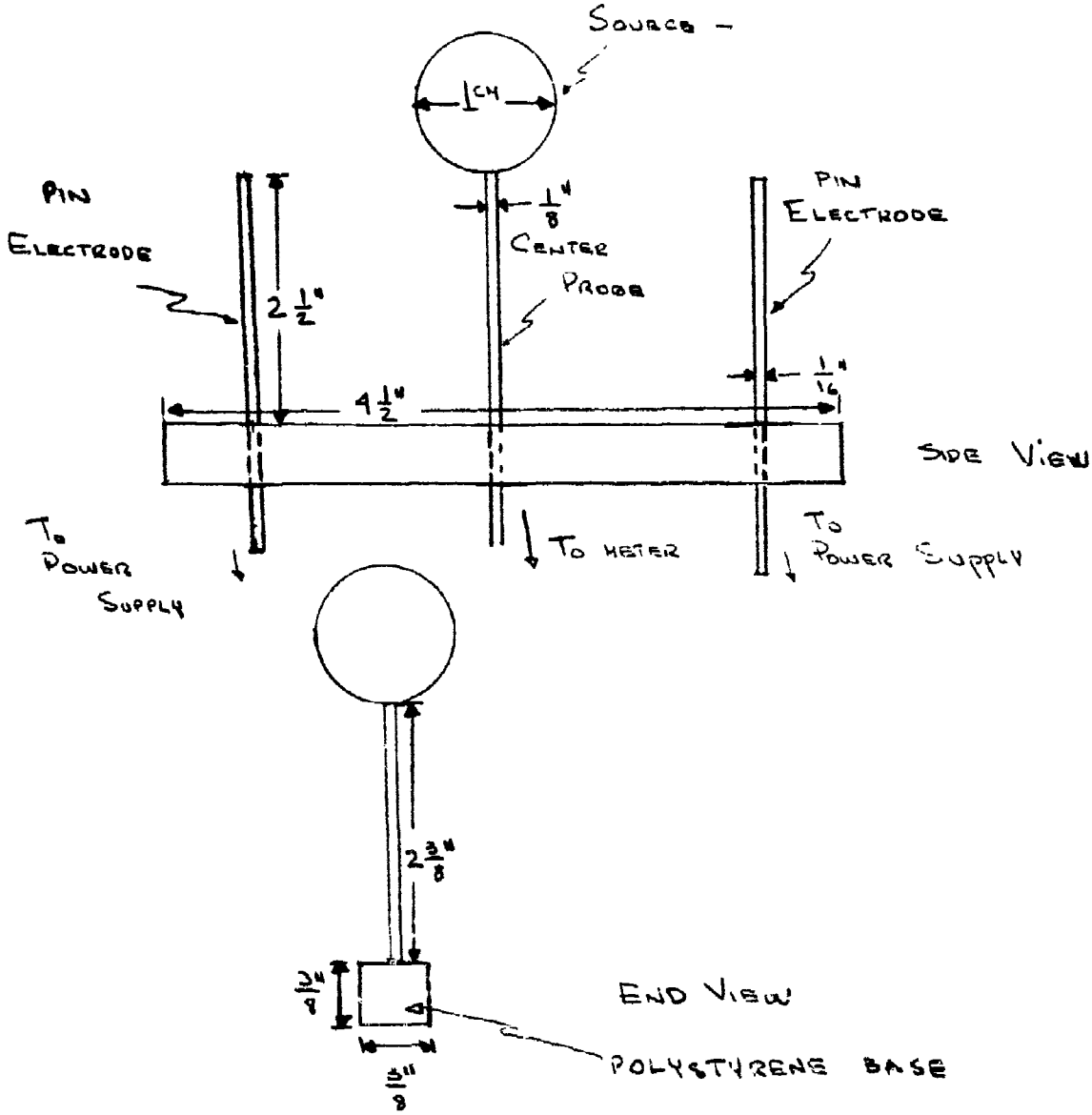

Pin Electrode Ion Anemometer

Mechanical Arrangement - Not to scale

Figure No. 6-1.

PIN ELECTRODE ION ANEMOMETER PERFORMANCE

TEST PARAMETER ; FIELD VOLTAGE

INSTRUMENT OUTPUT CURRENT VS INSTRUMENT VELOCITY

+ 1400 V ELECTRODE SPACING: $3\frac{3}{4}$"
⊙ 2850 V
⊡ 2000 V

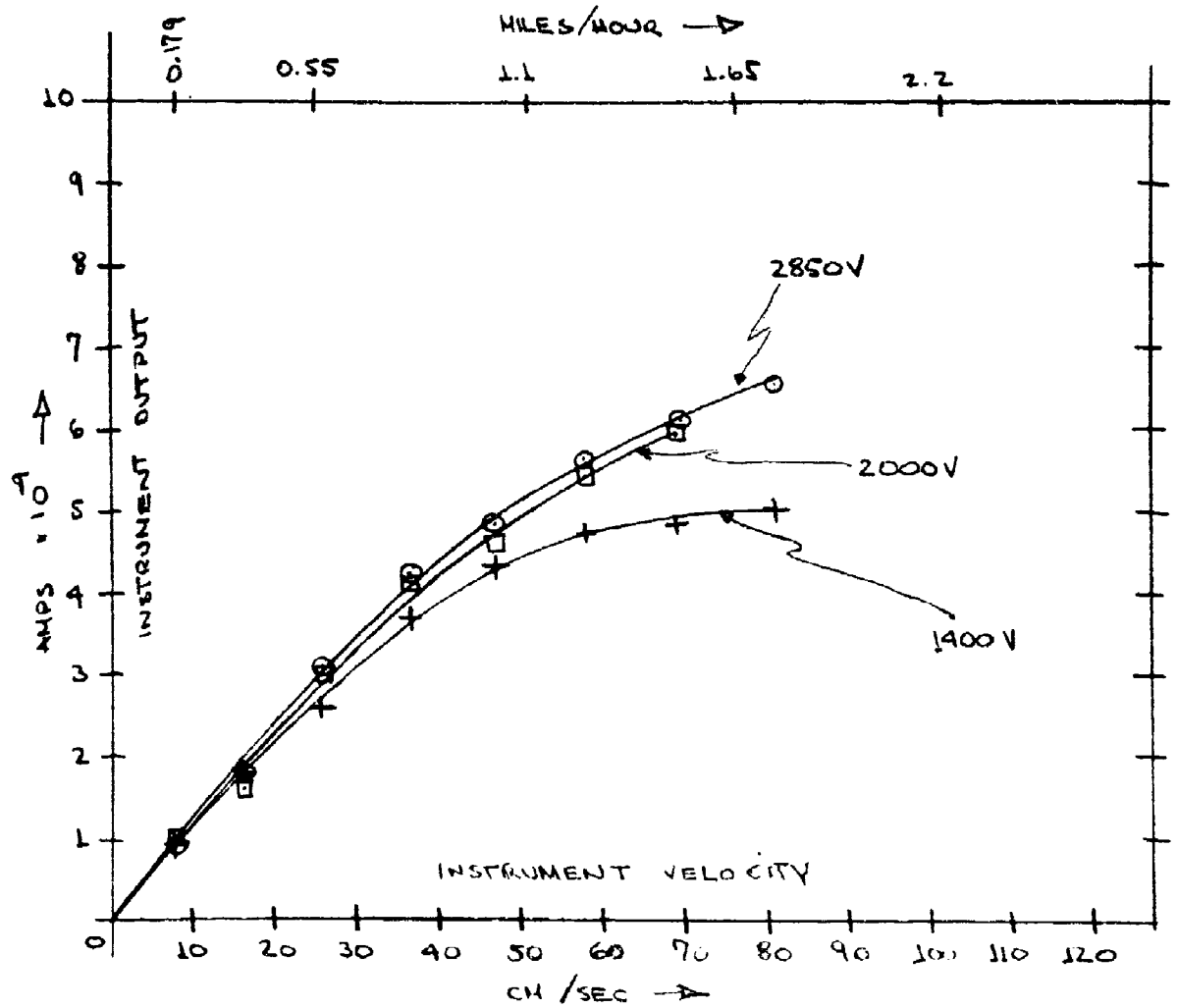

Fig No. 6-2

PIN ELECTRODE ION ANEMOMETER PERFORMANCE

TEST PARAMETER: ELECTRODE SPACING

INSTRUMENT OUTPUT CURRENT VS INSTRUMENT VELOCITY

□ $2\frac{5}{8}$" SPACE FIELD VOLTAGE 2000V

△ $1\frac{3}{4}$" "

× $3\frac{3}{4}$" "

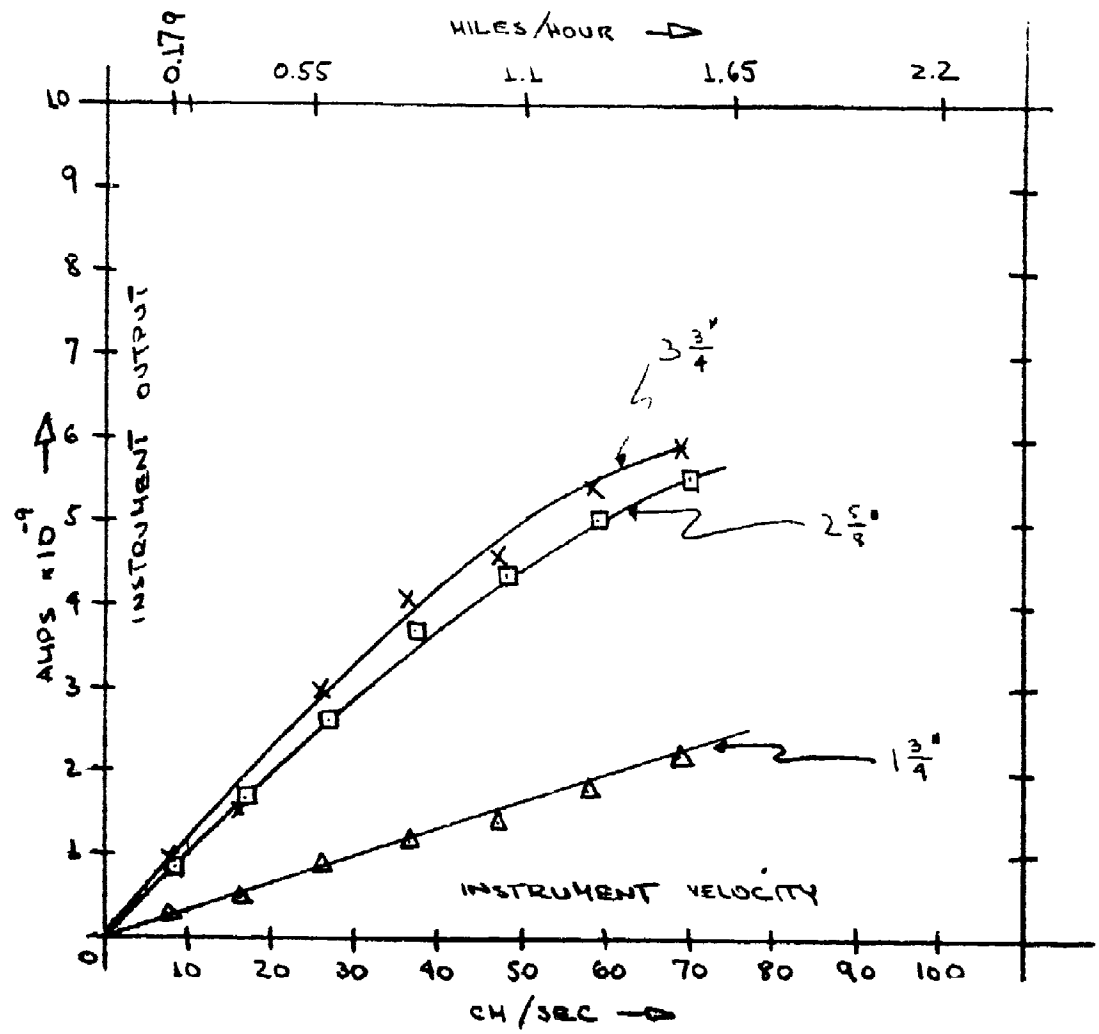

FIG. NO. 6-3

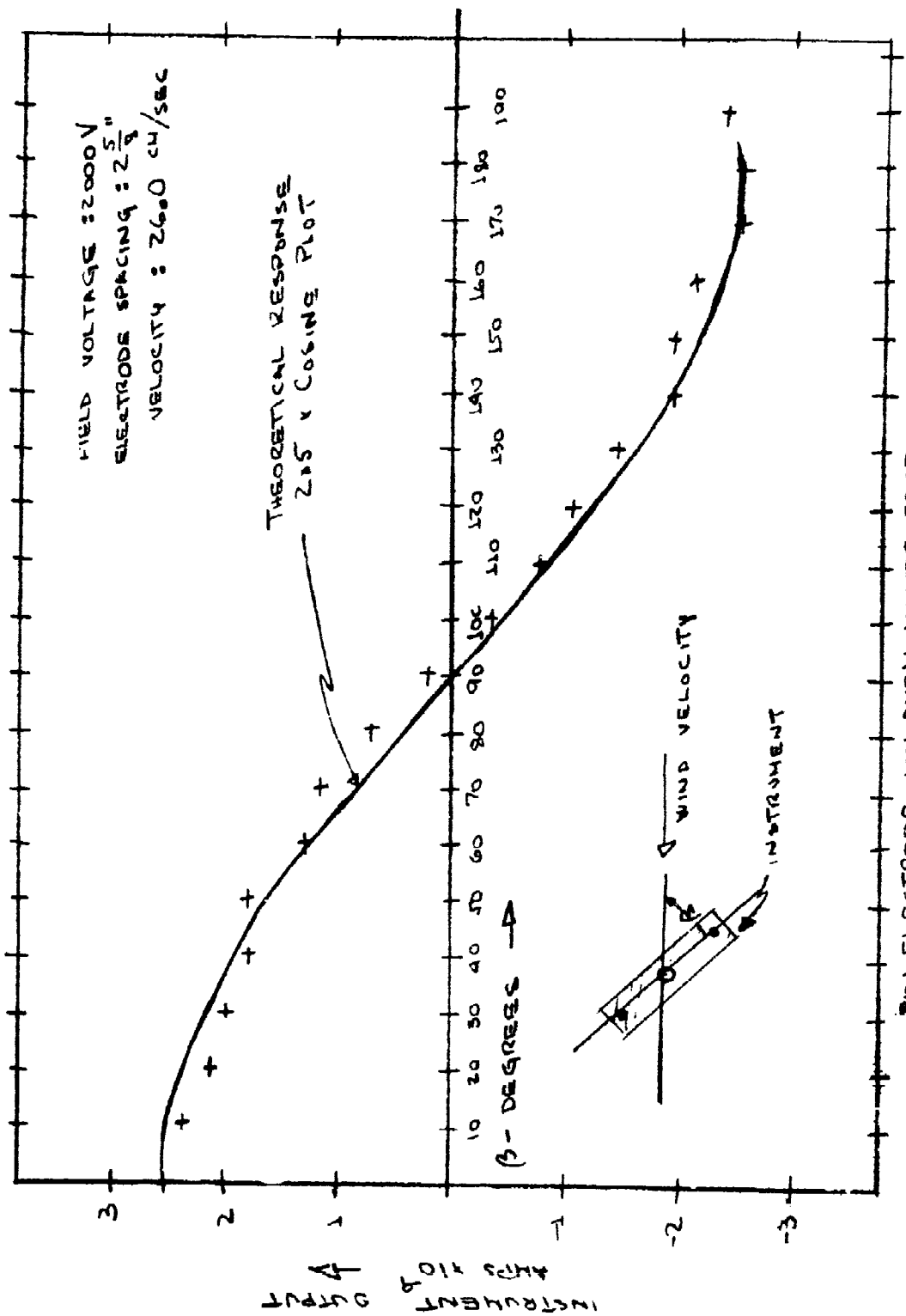

PIN ELECTRODE ION ANEMOMETER PERFORMANCE
TEST PARAMETER: ANGLE OF YAW

Fig No. 6-4

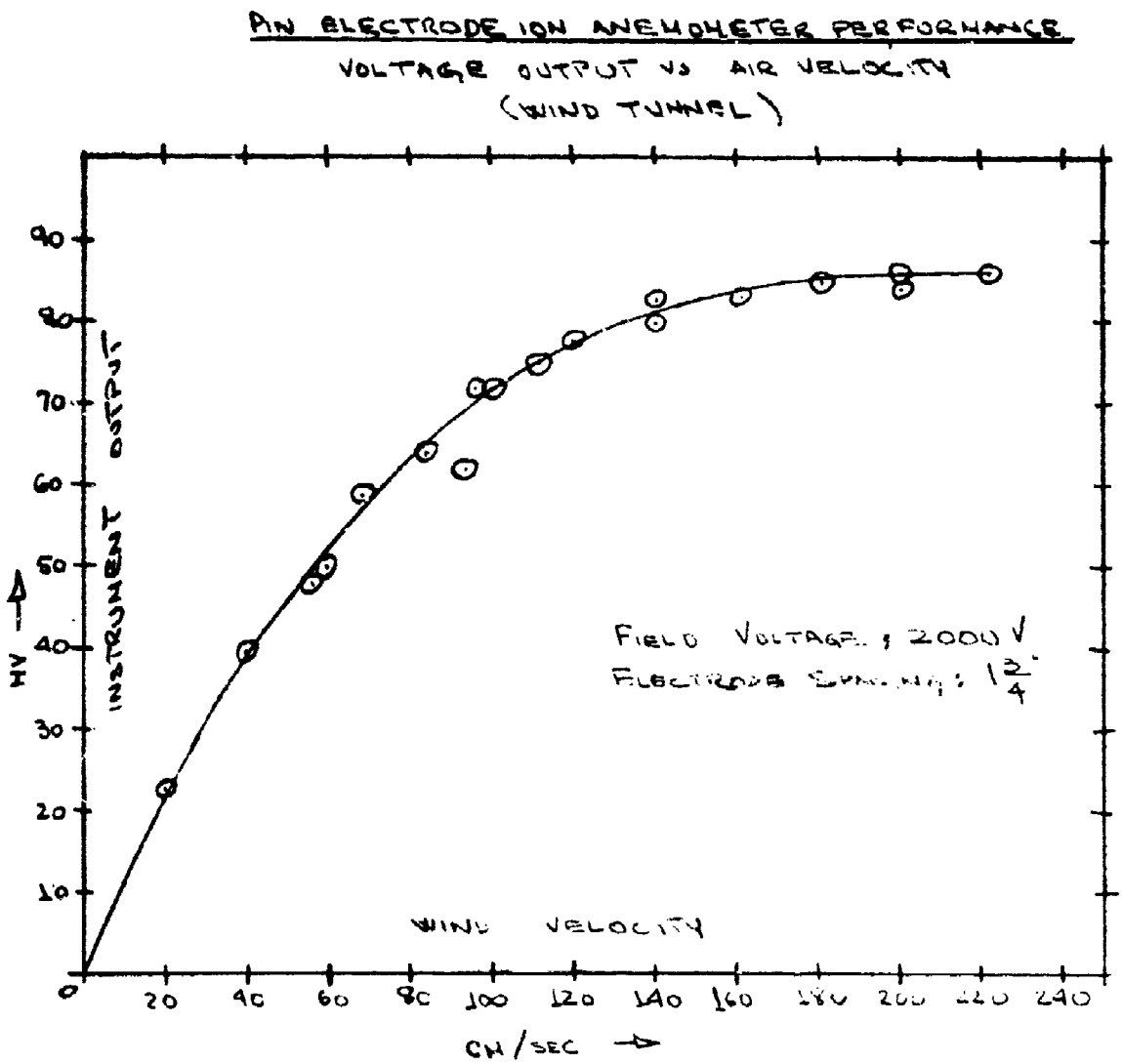
AN ELECTRODE ION ANEMOMETER PERFORMANCE
VOLTAGE OUTPUT VS AIR VELOCITY
(WIND TUNNEL)
INSTRUMENT OUTPUT
HV
0
10
20
30
40
50
60
70
80
90
20
40
60
80
100
120
140
160
180
200
220
240
WIND VELOCITY
CM/SEC
FIELD VOLTAGE : 2000 V
ELECTRODE SPACING : 1 3/4"

Fig No 6 5

to angled flow was determined within the horizontal plane embracing the sensitive axis, were satisfactory. A typical yaw characteristic curve is given in Figure 6-4.

The pin electrode configuration was ultimately rejected on the basis of a non-linear output at elevated velocities. Further attempts to achieve a linear output versus velocity relationship by increasing the field strength (through decreasing the electrode spacing and increasing the field voltage) were not successful in improving the "high speed" ($>$ 100 cm/sec.) performance. Consequently, despite the advantages of good yaw response and extreme mechanical simplicity, the pin electrode configuration was set aside.

B. Three Parallel Grids Configuration (See Figure 6-6)

The saturation effect observed in the pin electrode model was thought to have been the result of a non-uniform electric field in the space between the two outer electrodes. In order to obtain a more uniform electric field, the outer electrodes and the center probe, which had the shape of thin rods in the pin electrode configuration, were made in the form of three parallel meshes (grids). This was done in order to simulate the effect of three parallel plates and at the same time permit the flow of air through the instrument.

Using the basic configuration of three parallel grids, three variations were tested:

1) three coarse grids
2) three fine grids
3) two outer coarse grids and one center fine grid

The first of these variations was made (Cadmium plated steel, 4 squares to the inch) as shown in Figure 6-6. Figure 6-7 shows the instrument output current

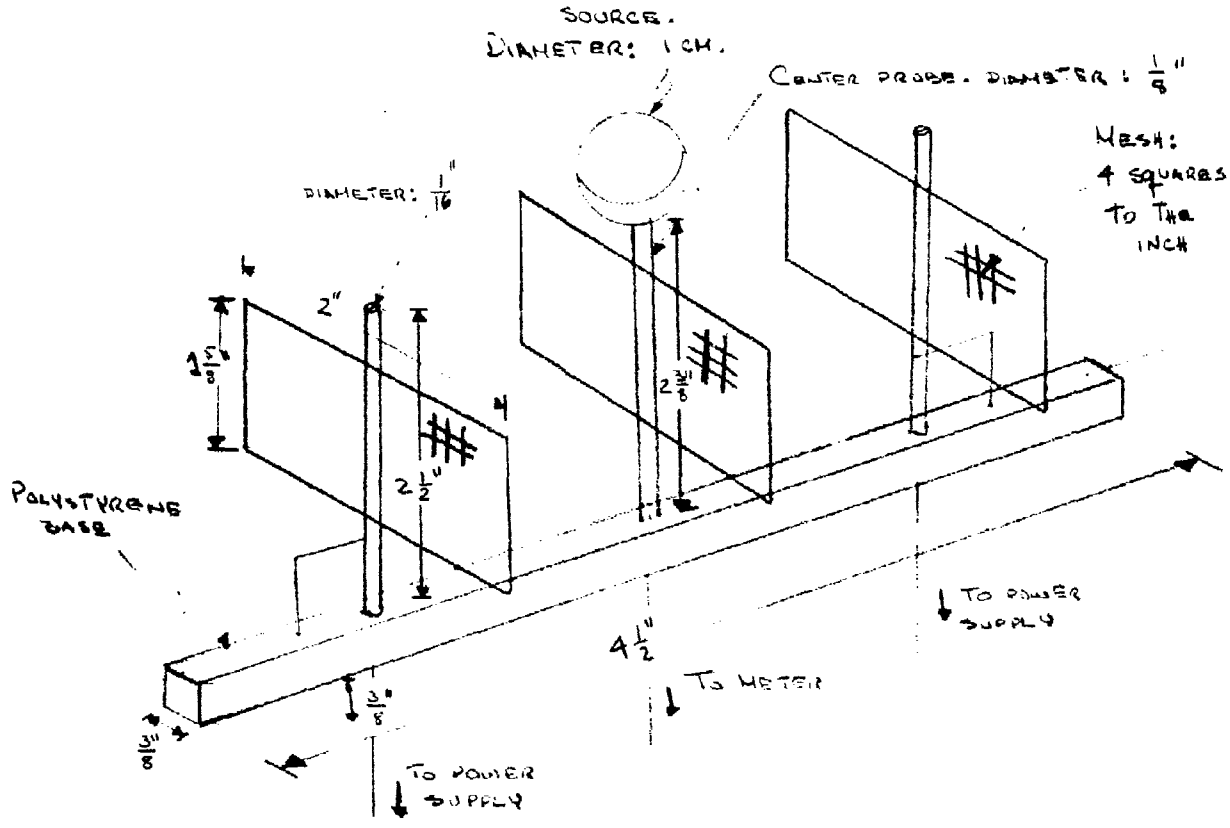

THREE PARALLEL COARSE GRIDS ION ANEMOMETER

MECHANICAL ARRANGEMENT - NOT TO SCALE

FIGURE No. 6-6

THREE PARALLEL COARSE GRIDS ION ANEMOMETER PERFORMANCE

OUTPUT CURRENT VS AIR VELOCITY

FIELD VOLTAGE: 2000 V

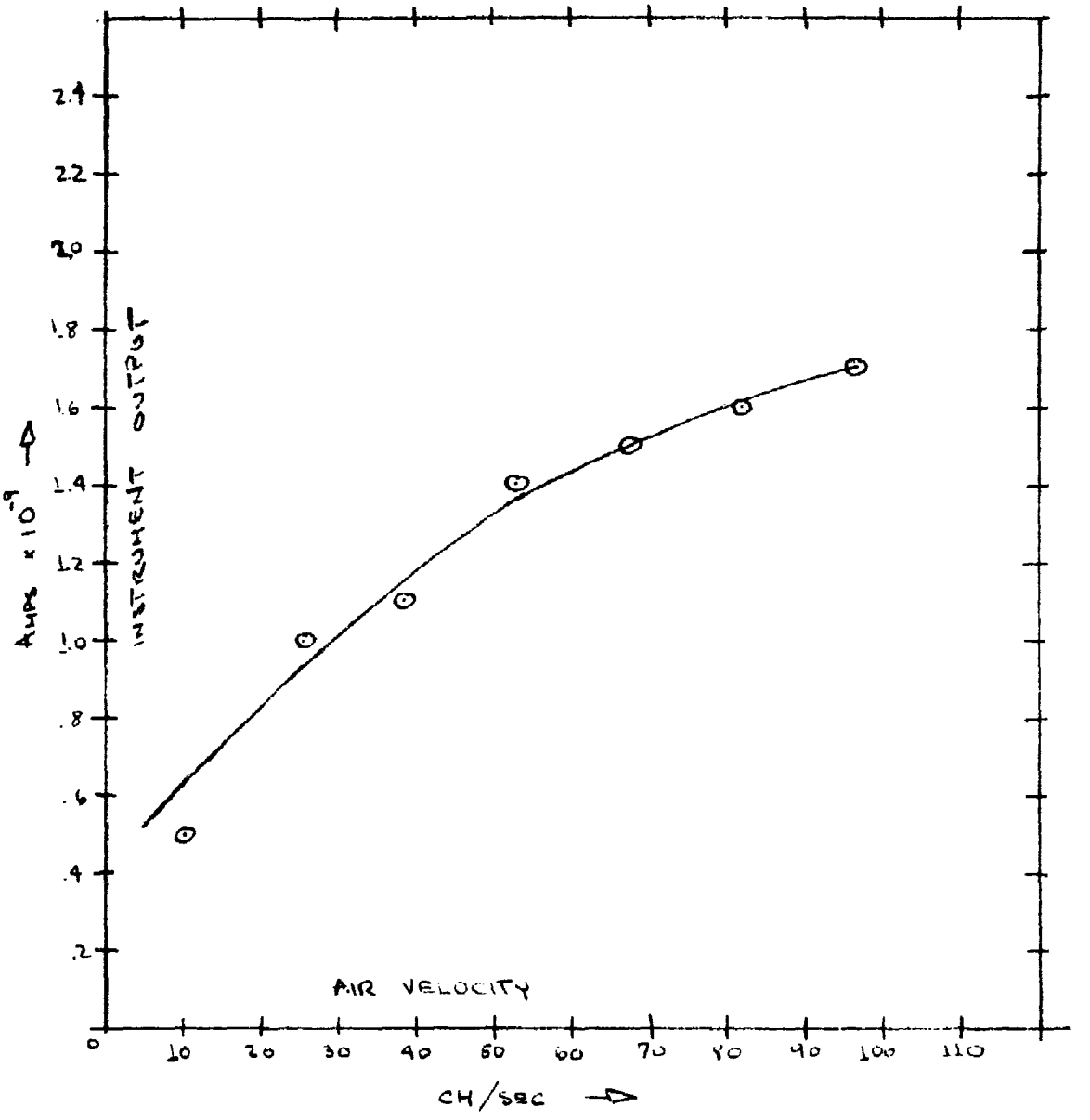

Fig No 6-7

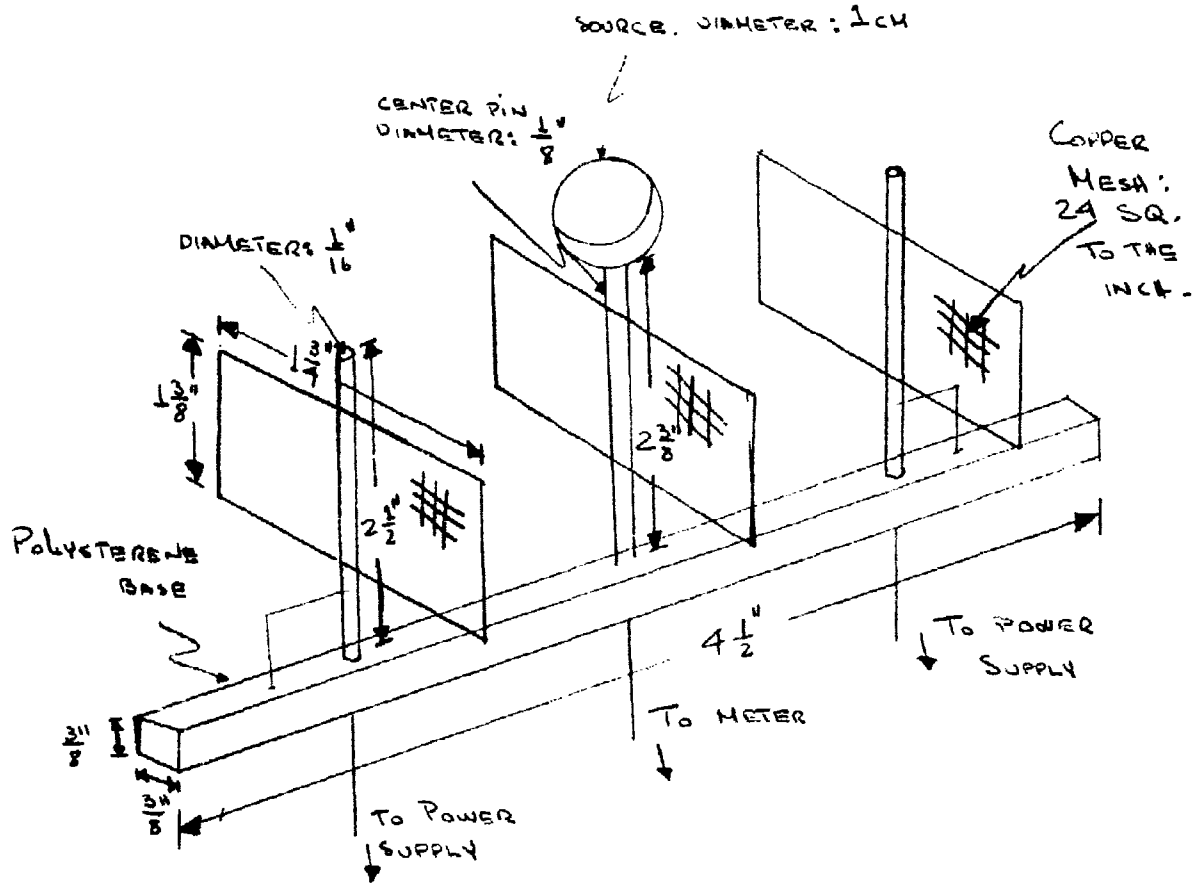

THREE PARALLEL FINE GRIDS ION ANEMOMETER

MECHANICAL ARRANGEMENT - NOT TO SCALE

FIGURE No. 6-B

(no amplification) against air velocity. It is observed that the resulting curve is not linear and still shows a "saturation" effect, similar to the response of the pin electrode configuration.

In order to improve the uniformity of the electric field in the space between the outer electrodes, these, as well as the center probe were changed, and replaced by a different mesh, this time a fine copper grid with a spacing of 24 to the inch (Figure 6-8). A test of the response to angled flow was made with this configuration. Figure 6-9 shows the instrument output in volts, using an operational amplifier (amplification of 15,000). This test was done using the insect tunnel at an air velocity of 266 cm/sec. Two field voltages were tested: 2000 V and 4000 V. The curves show the different levels of output sharing a similar trend. However, they did not exhibit a cosine response to angled flow.

The third variation of three parallel grids configuration was a combination of the last two models. The two other electrodes were made of coarse mesh while the center probe was a fine copper mesh (Figure 6-10). Figure 6-11 shows the instrument output measured in volts, again using an amplification of 15,000. The figure also shows a theoretical cosine curve. While demonstrating some improvement of the yaw test results over the prior configuration (Figure 6-9), the parallel grid concept was abandoned at this point.

The parallel grid arrangement was found to offer the same linearity difficulties (velocity versus output) as the pin electrode configuration and a mediocre yaw performance, considerably inferior to the pin electrode configuration. As there appeared to be no advantage gained by the parallel grid arrangement, it was set aside.

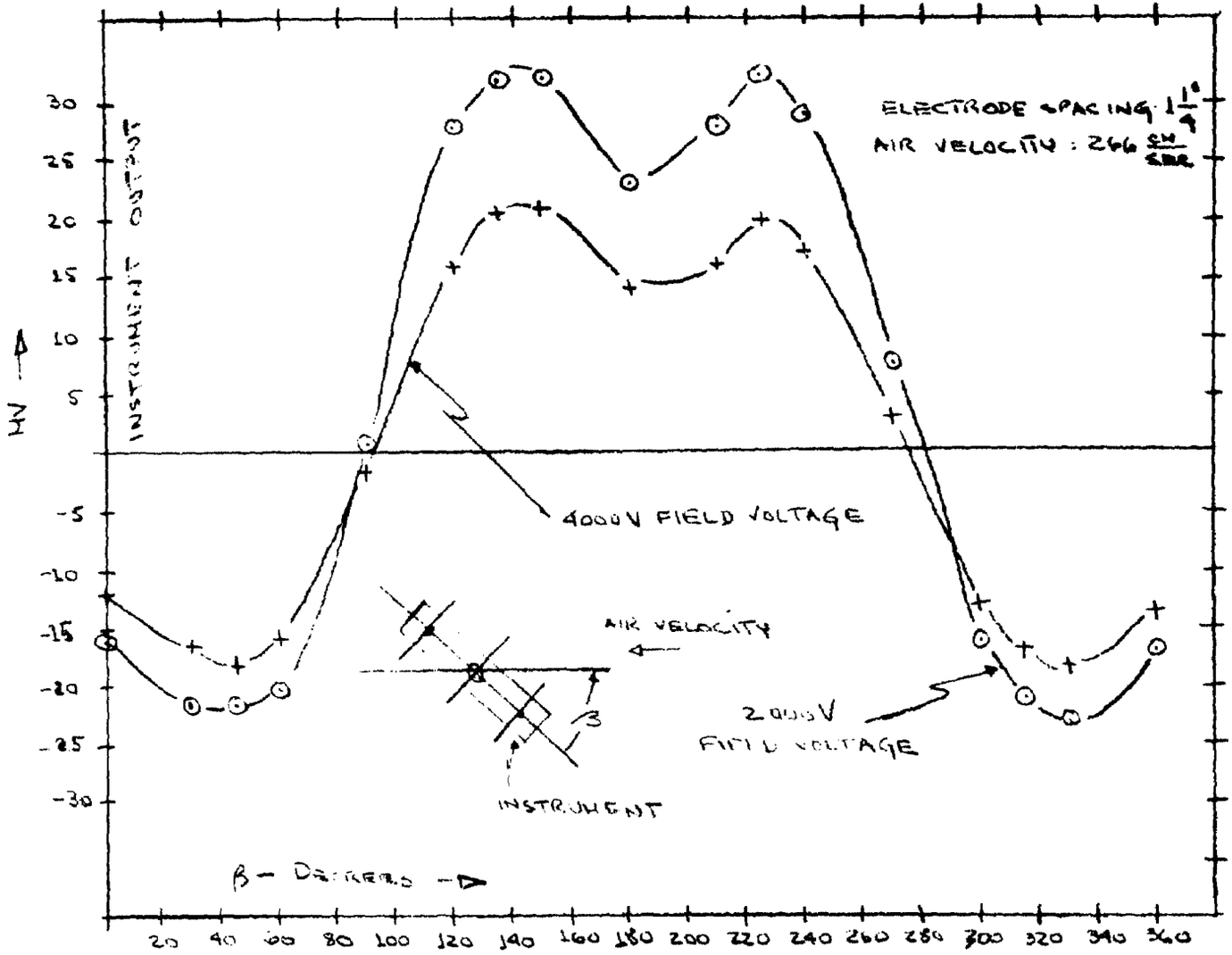

THREE PARALLEL FINE GRIDS ION ANEMOMETER PERFORMANCE
TEST PARAMETER : ANGLE OF YAW

FIG NO. 6-9

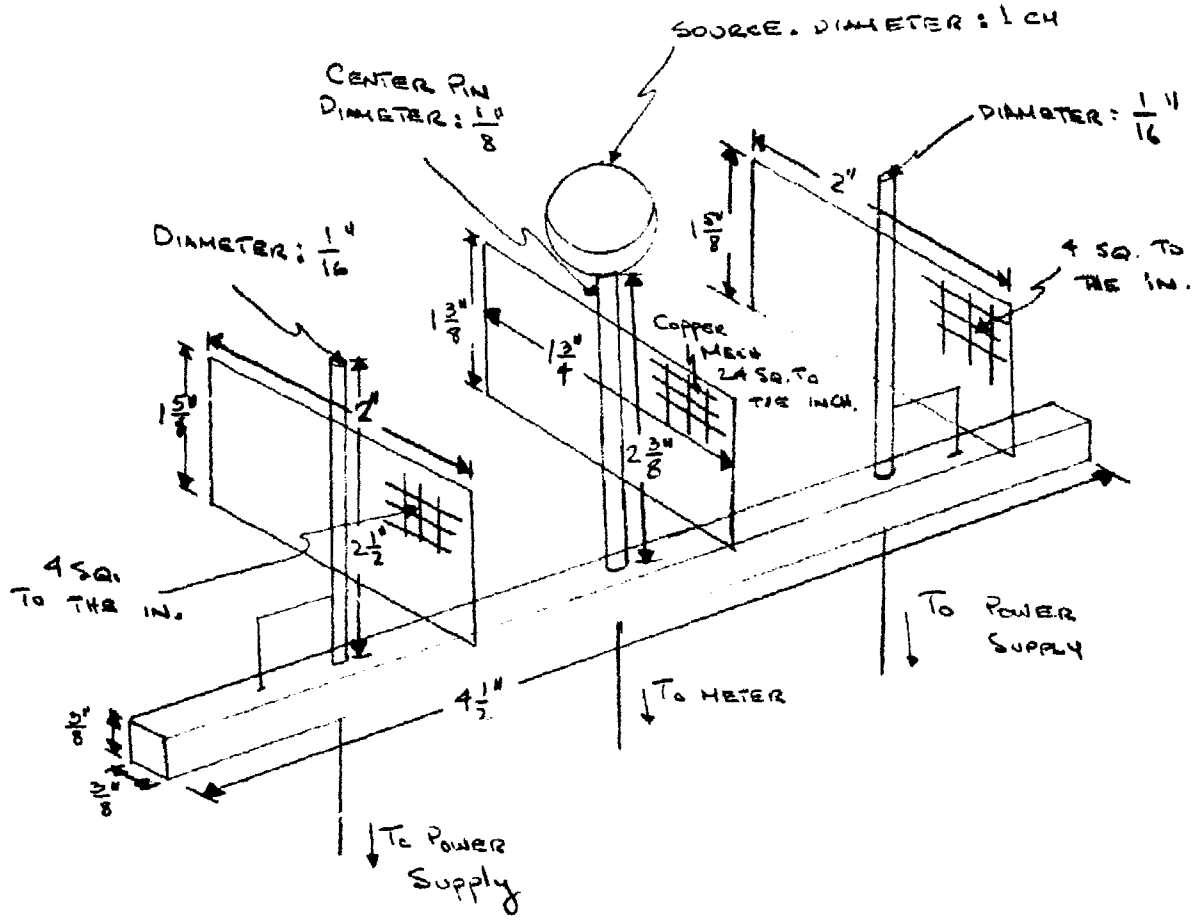

TWO COARSE GRID ELECTRODES AND A PARALLEL CENTER COPPER GRID

MECHANICAL ARRANGEMENT — NOT TO SCALE

FIG. 6-10

SPACINGS: $1\frac{1}{4}$", SPEED: 266 cm/sec

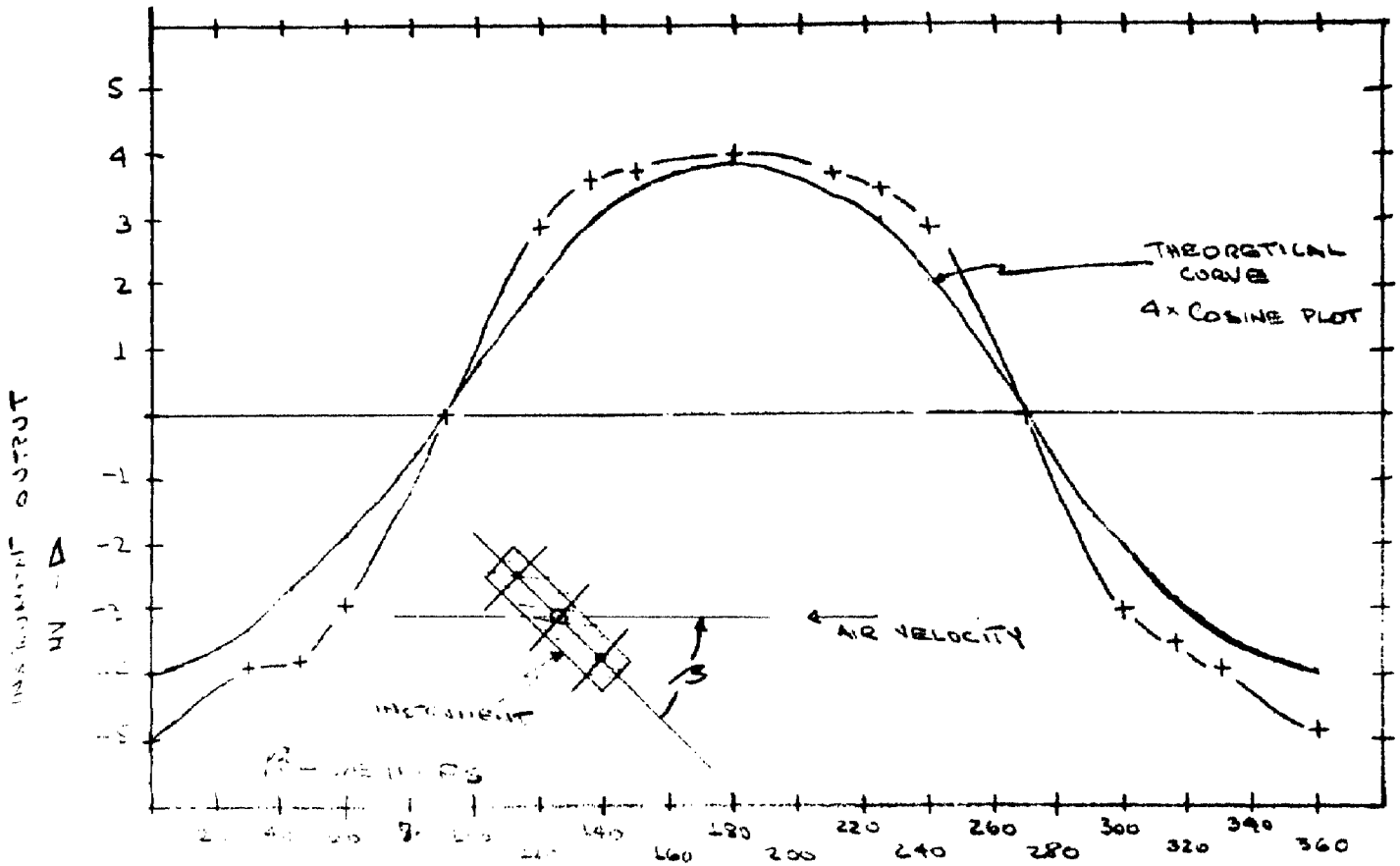

THIN COPPER WIRE ELECTRODES AND A PARALLEL CENTER COPPER GRID

IOM ANEMOMETER PERFORMANCE

TEST PARAMETER - ANGLE OF YAW

FIG No. 6-11

C. Cross Electrode Configuration (See Figure 6-12)

Noting that the previously described pin and grid electrodes each had certain desirable characteristics, albeit with certain drawbacks, an attempt was made to obtain a compromise external electrode in the form of a simple cross. It was hoped that such an electrode would demonstrate both the good yaw characteristics of the pin electrode plus the lateral distribution of field strength implicit in the grid electrode. The cross electrode has a vertical pin member to which is joined a horizontal arm .

Yaw test results for this model are given in Figure 6-13, depicting the response of the instrument (voltage amplified 15,000 times) to angled flow within the horizontal plane. The air velocity was 266 cm/sec., and the electrode spacing 1-1/4 inches. Two field voltages were tested (2000 V and 4000 V) resulting in differing outputs.

Noting that the yaw response differed considerably from the desired cosine value, and that the response was much inferior to that of the pin electrode, the cross electrode concept was set aside.

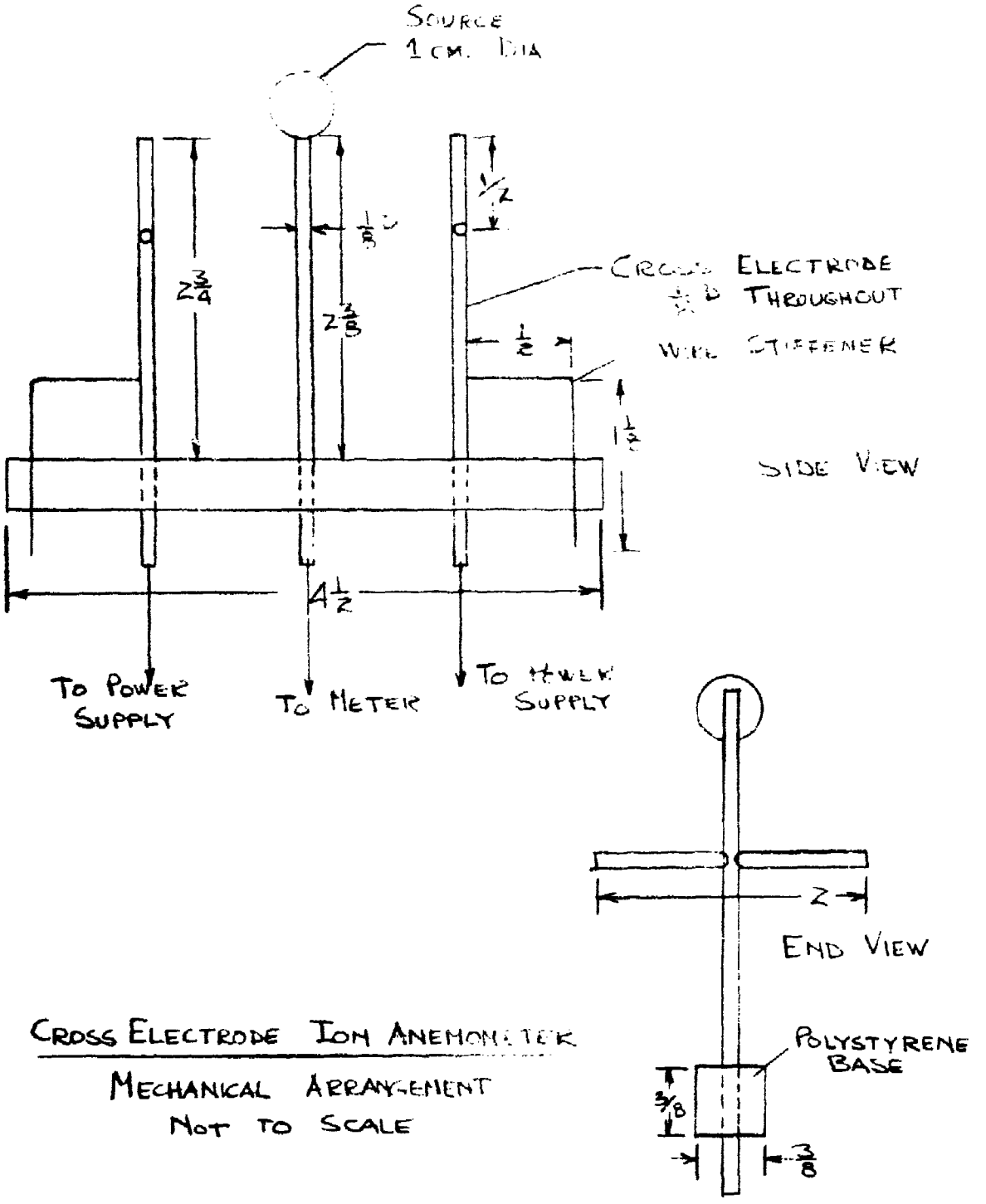

CROSS ELECTRODE ION ANEMOMETER

MECHANICAL ARRANGEMENT

NOT TO SCALE

FIG. NO. 6-12

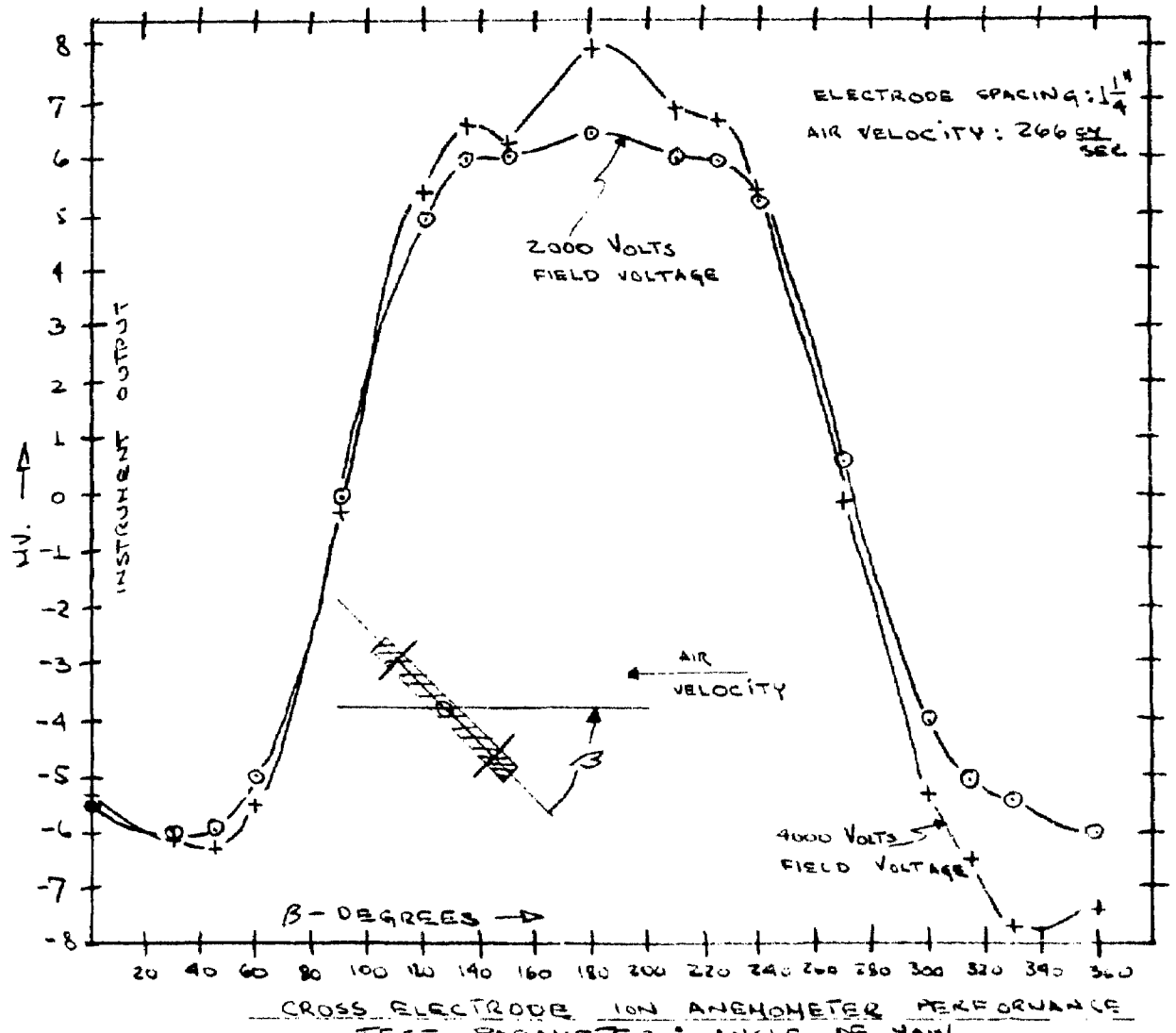

CROSS ELECTRODE ION ANEMOMETER PERFORMANCE
TEST PARAMETER: ANGLE OF YAW

FIG. NO. 6-13

Security Classification DUPLICATE

DOCUMENT CONTROL DATA - R & D

(Security classification of title, body of abstract and indexing annotation must be entered when the overall report is classified)

1. ORIGINATING ACTIVITY (Corporate author) New York University	2a. REPORT SECURITY CLASSIFICATION Unclassified 2b. GROUP N/A

3. REPORT TITLE

Ion Anemometer

4. DESCRIPTIVE NOTES (Type of report and inclusive dates)

Final Report No 1530-02

5. AUTHOR(S) (First name, middle initial, last name)

Alan M. Nathan
Leon Bennett
Moises Cytter

6. REPORT DATE	7a. TOTAL NO. OF PAGES	7b. NO. OF REFS
October 1969	65	

8a. CONTRACT OR GRANT NO.	9a. ORIGINATOR'S REPORT NUMBER(S)
DAAB07-68-C-0396	
b. PROJECT NO.	1530-02
c.	9b. OTHER REPORT NO(S) (Any other numbers that may be assigned this report)
d.	Ecom 0396 F

10. DISTRIBUTION STATEMENT

This document is subject to special export controls and each transmittal to foreign governments or foreign nationals may be made only with prior approval of CG, US Army Electronics Command, Ft Monmouth, NJ 07703 ATTN: AMSEL-BL-FM-P

11. SUPPLEMENTARY NOTES	12. SPONSORING MILITARY ACTIVITY
	US Army Electronics Command Fort Monmouth, New Jersey 07703 ATTN: AMSEL-BL-FM-P

13. ABSTRACT

An ion anemometer is described that is designed to measure one vector component of air velocity in the range from 0 to 120 cm/sec. The instrument's electrical output signal is a measure of the magnitude of the projection of the instantaneous wind vector onto the instrument's single axis of sensitivity. Ganging of more than one device permits the determination of two or three vectors components of the wind velocity.

The instrument employs a radioactive source of alpha particles to ionize the air molecules in a small region between two oppositely charged electrodes. The equal numbers of positive and negative ions generated at a constant rate are separately collected by the two charged electrodes. In the absence of wind, the potential due to space charge is zero at the electrical midpoint between the two collecting electrodes where an electrical probe is situated. Any wind component along the axis, however , causes an unbalance which is sensed by a small current in the probe that is amplified and recorded.

This development effort differs from prior work in its concentration on the following goals: 1) linear output with velocity, 2) a true cosine law response to an off-axis airstream, 3) a usefully large analog signal capable of simple readout at very low wind speeds.

DD FORM 1 NOV 68 1473 REPLACES DD FORM 1473, 1 JAN 64, WHICH IS OBSOLETE FOR ARMY USE.

Security Classification

14. KEY WORDS	LINK A		LINK B		LINK C	
	ROLE	WT	ROLE	WT	ROLE	WT
1. anemometry						
2. low wind speed measurements						
3. met instrumentation						
4. ion anemometer						